Final Report

NASA CR-111916

AN INVESTIGATION OF MOUNTAIN WAVE TURBULENCE WITH LIDAR OBSERVATIONS

By: WILLIAM VIEZEE

Prepared for:

NATIONAL AERONAUTICS AND SPACE ADMINISTRATION
LANGLEY RESEARCH CENTER
LANGLEY STATION
HAMPTON, VIRGINIA 23365

CONTRACT NAS1-9951

STANFORD RESEARCH INSTITUTE
Menlo Park, California 94025 · U.S.A.

STANFORD RESEARCH INSTITUTE
Menlo Park, California 94025 · U.S.A.

Final Report

NASA CR-111916

April 1971

AN INVESTIGATION OF MOUNTAIN WAVE TURBULENCE WITH LIDAR OBSERVATIONS

By: WILLIAM VIEZEE

Prepared for:

NATIONAL AERONAUTICS AND SPACE ADMINISTRATION
LANGLEY RESEARCH CENTER
LANGLEY STATION
HAMPTON, VIRGINIA 23365

CONTRACT NAS1-9951

SRI Project 8573

Approved by:

R. T. H. COLLIS, *Director*
Aerophysics Laboratory

RAY L. LEADABRAND, *Executive Director*
Electronics and Radio Sciences Division

ABSTRACT

In March and April of 1969 and 1970, lidar (laser radar) observations of the atmospheric structure were made in the lee of the Sierra Nevada during the occurrence of mountain lee waves. Rawinsonde ascents and, on some occasions, research-aircraft flights supported the lidar observations. The objective of the program was to explore the applicability of the lidar technique to atmospheric turbulence detection. The observations demonstrate that the lidar can delineate significant features of the atmospheric-flow pattern by monitoring echoes from concentrations of particulate matter that characterize the airflow structure in the form of either visible or subvisible clouds and dust. For example, the lidar describes in remarkable detail (1) the development, spatial distribution, and optical characteristics of the lenticular clouds that identify the tropospheric layer of major wave motion and (2) the formation and location of rotor clouds, which identify the lower turbulence zone. By monitoring in space and time the echoes that arise from the presence of the rotor clouds and from the presence of dust and variable dust concentrations within the boundary layer, the lidar can detect the vertical extent and the temporal variations of the lower turbulence zone (the Turbulent Boundary Layer under the lenticular clouds), which can harbor moderate and severe turbulence associated with convection and rotor flow.

No evidence of the presence of significant turbulence was found within the midtropospheric layer of the lenticular clouds. At all times, the lidar data show a wave cloud structure and organization reflecting highly laminar flow. The presence of turbulence in the upper troposphere above the wave clouds cannot be explored directly by a ground-based lidar because the lenticular clouds are frequently opaque to the lidar

pulse energy, especially during low-level wave development when the wave clouds consist of water droplets. However, there is evidence that, indirectly, information on turbulence can be inferred from the structure and location of the wave clouds as detected by the lidar. For example, observations of an intense wave in the lee of Mt. Rose on 24 April 1970 suggest that the probability of the presence of turbulence above the wave clouds becomes high when the wave cloud system propagates downwind from the mountain crest accompanied by pronounced vertical stacking of the lenticular clouds (these features are characteristic of lee wave intensification). The increase in turbulence probability is inferred from rawinsonde data that show the development in time of narrow layers of low Richardson number ($\ll 0.25$) between 25,000 ft and 40,000 ft MSL. On the basis of all data collected, it is concluded that the mountain lee wave provides a natural laboratory for the study of wave-generated turbulence, the relating of turbulence to low Richardson number, and the extent to which atmospheric flow patterns can be delineated by lidar.

ACKNOWLEDGEMENTS

Personnel of the Aerophysics Laboratory at SRI who contributed to the work described in this report included Mr. Ronald T. H. Collis, Director of the Aerophysics Laboratory, who planned and supervised the overall experiment; Mr. Roy M. Endlich, Manager of the Weather Dynamics Group, who assisted in the field operation and supervised the rawinsonde data-collection program; and Mr. John Oblanas, Research Engineer, who coordinated the preparation of lidar and data recording equipment. The active field crew consisted of Messrs. Norm Nielsen, William Dyer (lidar operation and maintenance), and Albert Smith (rawinsonde operation and maintenance). Special recognition is given to the personnel from the NASA Flight Research Center at Edwards, California who provided the supporting program of aircraft observations in the southern Sierra Nevada under the direction of Mr. L. J. Ehernberger.

The author expresses his gratitude to Drs. Harold E. Klieforth and John Hallett of the Desert Research Institute at Reno, Nevada who arranged the use of a suitable field site along the Mt. Rose Highway and advised us in planning and conducting the experiment in the northern Sierra Nevada. We are indebted to Dr. J. D. Lawrence, NASA Langley Research Center, for his encouragement and support of this work.

CONTENTS

ILLUSTRATIONS

ILLUSTRATIONS (Continued)

ILLUSTRATIONS (Continued)

TABLES

I INTRODUCTION AND OBJECTIVES

The development of wave motion in a stably stratified airflow crossing a mountain barrier is well documented and formulated in the literature on the basis of theoretical studies and observational programs (e.g., Corby, 1954; Alaka, 1960; Foldvik and Wurtele, 1967).* A mountain barrier of major importance in the generation of such wave motion is the Sierra Nevada; its lee waves were the subject of intensive investigation during the well-known Sierra Wave Project (Holmboe and Klieforth, 1957).

It is in connection with high-level turbulence investigations that studies of the atmospheric structure in the lee of mountains have been resumed in recent years (Kuettner and Lilly, 1968; Wooldridge and Lester, 1969). High-level turbulence is known to be associated with mountain barriers and mountain lee waves (Reiter and Foltz, 1967; Harrison and Sowa, 1966). Furthermore, it is currently believed (e.g., Atlas et al. 1970; Roach, 1970) that clear air turbulence other than that produced by convection (e.g., thunderstorms) is generated by gravity waves. Since the mountain wave is a system of quasi-stationary gravity waves, the lee of a mountain barrier provides a natural laboratory for investigating wave-generated turbulence.

The general objective of the study conducted under the contract was to evaluate the potential of lidar (the optical equivalent of radar) to describe the atmospheric structure in the lee of a mountain barrier during the occurrence of lee waves. The particular objective was to establish to what extent lidar observations (from the ground, as in this study, or subsequently from an aircraft) can be used to delineate or interpret the airflow for the detection or anticipation of turbulence.

---

*References are listed at the end of the report.

II SUMMARY AND CONCLUSIONS

In order to achieve the contract objectives, a series of lidar observations and supporting rawinsonde ascents were made in the southern Sierra Nevada in the lee of Lone Pine Peak (12,944 ft MSL) during March and April 1969, and also in the northern Sierra Nevada in the lee of Mt. Rose (10,778 ft MSL) during March and April 1970. Lidar observations were made from a location in the lee at time periods during which the presence of waves was evident from the presence of lenticular clouds and/or rotor clouds. During the southern Sierra Nevada experiment, subjective turbulence observations were made by a research aircraft from the NASA Flight Research Center at Edwards, California. Unfortunately no such aircraft was available during the experiment in the northern Sierra Nevada, but turbulence conditions were inferred from values of the Richardson number computed from the data of radiosonde balloons released from a location 18 miles upwind from the lidar site.

Although plans to assemble and transport personnel and equipment are readily made on the basis of the Sierra-wave climatology,* the success of the experiment depended entirely on the upper-air circulation that existed after personnel and equipment had been transported to a predetermined field site. The wave situations that could be monitored in the southern Sierra Nevada during March and April 1969 did not exceed moderate intensity because of the absence of a high-velocity jet stream. In the northern Sierra Nevada a single lee wave of moderate intensity was observed on 13 March 1970, after which a persistent, high-pressure ridge over the western U.S. blocked further wave development for a period of four consecutive weeks. After the high-pressure ridge broke

*The expected frequency of occurrence of days with lee waves is about 30 percent during March and April (about 2 days per 7-day week).

down, a strong wave was observed and recorded on 24 April 1970.

Detailed analyses and discussions of the lidar, rawinsonde, and turbulence data obtained in the southern Sierra Nevada near Lone Pine are presented in Scientific Report 1 (Viezee, 1970). The present final report summarizes the entire lidar/mountain-wave observation program.

The data collected during the study extend and clarify the lidar observations of Sierra-wave conditions made initially by Collis et al. (1968) at Independence, California, during February and March 1967. In terms of the general objective, it is found that the lidar can outline various features of the atmospheric structure during mountain-wave conditions. In particular, it describes in remarkable detail the location, spatial distributions, and optical characteristics of the lenticular clouds, and the development and location of rotor clouds. Information on the lower turbulence zone (the Turbulent Boundary Layer under the lenticular clouds) supplied by the lidar is based on echoes that arise from the presence of rotor clouds and from the presence of dust and variable dust concentrations within the boundary layer. In terms of the particular objectives of the program, it is concluded that a ground-based lidar can detect the vertical extent and the temporal variations of the lower turbulence zone, which can harbor moderate and severe turbulence associated with convection and rotor flow.

No evidence of the presence of significant turbulence was found in the midtropospheric layer of the lenticular clouds. At all times, the lidar data show a wave cloud structure reflecting highly laminar flow. The presence of turbulence in the upper troposphere above the wave clouds cannot be explored directly by a ground-based lidar because the lenticular clouds are frequently opaque to the lidar pulse energy, especially during low-level wave development, when the wave clouds consist of water droplets. However, there is evidence that, indirectly, information on turbulence can be inferred from the structure and location of the wave clouds as detected by the lidar. For example, observations of an intense wave in the lee of Mt. Rose on 24 April 1970 suggest that

the probability of the presence of turbulence above the wave clouds becomes high when the wave cloud system propagates downwind from the mountain crest accompanied by vertical stacking of the lenticular clouds (these features are characteristic of lee-wave intensification). The increase in turbulence probability is inferred from rawinsonde data that show the development in time of narrow layers of low Richardson number (< 0.25) between 25,000 ft and 40,000 ft MSL.

The potentially turbulent areas identified from the observation program (e.g., the lower turbulence zone under the wave clouds and the upper turbulence zone above the wave clouds) are compatible with the mountain-wave turbulence observations discussed by Kuettner (see Chapters 10 and 11 in Holmboe and Klieforth, 1957).

The air-cooled ruby lidars used in the program until January 1971 had relatively low firing rates (1 pulse per minute) when operated under the frequently adverse field conditions that were encountered. Consequently, the lee-wave structure analyzed from data of horizon-to-horizon scans had a low time resolution and could only be interpreted in terms of the gross, time-integrated features of the mountain wave.

A greatly improved mobile lidar system, the SRI/APCO Mk VIII lidar, has recently become available for field use. This ruby system is liquid-cooled, has a high pulse-repetition rate (20 to 30 pulses per minute), and includes an automatic programmed scanning and firing capability. The backscatter data received after each lidar pulse transmission are stored on a magnetic disc. After each horizon-to-horizon scan the backscatter data can be "played back" on an oscilloscope in the form of a range-corrected, intensity-modulated range-height indicator (RHI) display. Thus, vertical cross sections of atmospheric structure can be generated in near real time. The applicability of this highly automated system to mountain-wave turbulence observations* was explored in the lee of Mt. Rose, Nevada, during a one-week period in February 1971.

*Permission to use the Mk VIII lidar under the contract was granted by the Division of Meteorology of the Air Pollution Control Office, Environmental Protection Agency.

III TECHNIQUES OF OBSERVATION AND DATA ANALYSIS

The development of lidar, the optical equivalent of radar, has introduced a new remote atmospheric-probing technique. A pulsed laser in the visible or near infrared spectrum can remotely detect particulate matter of much smaller size and much lower concentration than can be seen by the human eye or "seen" by a microwave radar. Lidar, therefore, can be used to detect aerosol concentrations in the visually clear air, and can also map the spatial extent and temporal variations of tenuous and small-particle clouds. This new capability has led to the suggestion that lidar be used to detect clear-air turbulence. A reasonable approach appears to be the identification of the general airflow pattern from lidar observations of particulate matter, with the subsequent recognition of areas prone to turbulence that are present or may develop in the flow conditions in question (Collis, 1964). During the past two years this approach was applied under Contracts NAS1-8933 and NAS1-9951 to an investigation of atmospheric turbulence in mountain waves. Observations of the atmospheric structure during mountain-wave conditions were made in the lee of the Sierra Nevada with mobile lidar units. Figure 1 shows such a unit in operation during the mountain-wave observation program near Lone Pine, California. Three different ruby lidars were used during the course of the contracts. The mountain-wave observations in the southern Sierra Nevada were made with the SRI Mk V air-cooled lidar, the characteristics of which are listed in Table 1. The Mk VII lidar was used during the experiment in the northern Sierra Nevada in March and April 1970. Its characteristics are identical to those of the Mk V except that the 6-inch Newtonian reflecting telescope of the transmitter optics is replaced by a 2-inch refracting lens. This modification,

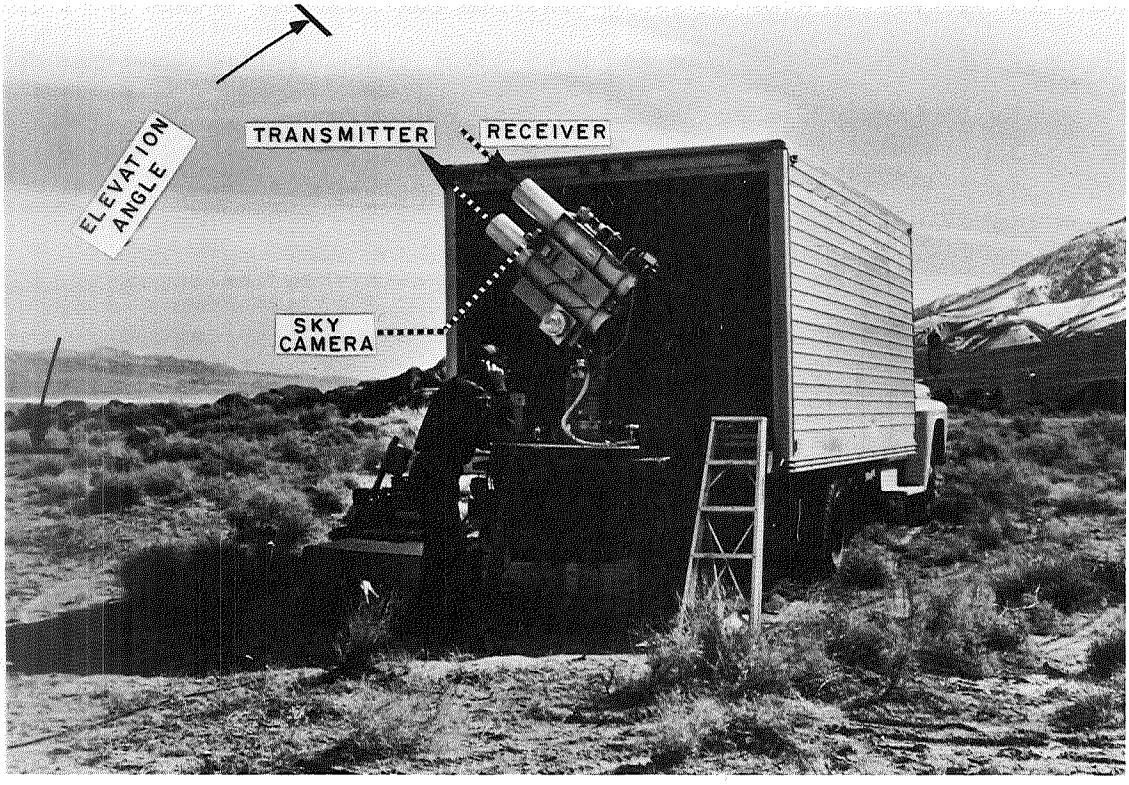

FIGURE 1 MOBILE LIDAR UNIT USED DURING MOUNTAIN-WAVE OBSERVATION PROGRAM IN THE SOUTHERN SIERRA NEVADA

Table 1

CHARACTERISTICS OF MARK V RUBY LIDAR

Transmitter	
Laser Material	Ruby
Wavelength	6943 Å
Energy output per pulse	0.22 joule
Pulse duration	15 nanoseconds
Peak power	15 megawatts
Aperture	6-inch Newtonian telescope
Beam divergence	0.3 mrad
Cooling	Forced air
Q-switch	Rotating prism and saturable dye
Receiver	
Aperture	6-inch Newtonian telescope
Effective aperture area	0.01 m^2
Solid angle of view	Adjustable, 0.5 to 4.0 x 10^{-3} radian
Filter bandwidth (3-dB attenuation)	13 Å
Photomultiplier	RCA 7265 (S-20 cathode)
Display	Tektronix Model 555 dual beam CRO (bandwidth = 30 MHz) with P-11 Phosphor; Polaroid camera, Type 410 film; Logarithmic response video amplifier (optional)

which was accomplished for the purpose of eliminating any interference of the field stop with the outgoing pulse shape, changes the transmitter beam divergence from 0.3 to 0.5 milliradian. A final experiment made in the lee of Mt. Rose, Nevada, in February 1971 involved the use of the SRI/APCO Mk VIII liquid-cooled ruby lidar. The characteristics of this greatly improved system are listed in Table 2.

Observations of atmospheric structure were made by firing the lidar at selected intervals in elevation angle while scanning from horizon to horizon in a vertical plane perpendicular to the mountain range. The state of the sky within the field of view of the lidar receiver was monitored by visual observation and by a sky camera mounted on the lidar unit (see Figure 1). On the basis of the visual observations and the photographs from the sky camera, received lidar echoes were attributed to returns from a visually clear sky, from tenuous (visually transparent) clouds, or from dense (visually opaque) clouds.

When using the Mk V or Mk VII lidar, the atmospheric backscatter signals from each transmitted pulse were monitored as functions of range on an oscilloscope and recorded on Polaroid photographs. The individual lidar backscatter signals from each complete vertical scan were used to construct by a hand-analysis technique two-dimensional cross sections of the atmosphere analogous to the familiar RHI presentation of weather radar practice. The cross sections were constructed by indicating along each line of elevation the range intervals over which significant lidar-return signals were recorded. Details on thickness and layered structure of the recorded echoes were obtained from a dual-beam oscilloscope display that showed the lidar echoes on an expanded time (range)-scale.

The pulse-rate frequency of the Mk V and Mk VII ruby lidars does not exceed 1 pulse per minute when the lidars are operated over extended time periods under adverse field conditions. Such relatively low PRF

Table 2

CHARACTERISTICS OF SRI/APCO MARK VIII LIDAR

Transmitter	
Laser rod	Ruby (3/8 x 3 inches)
Wavelength	6943.0 ± 0.4 Å
Beamwidth	0.8 mrad
Optics	Lens (2-inch), coaxial with receiver telescope
Pulse energy	0.9 joule
Pulse length	30 nanoseconds
Peak power	30 megawatts
Q-switch	Pockels cell
Maximum PRF	30 pulses/min
Cavity cooling	Refrigerated water
Receiver	
Optics	Newtonian reflector (6-inch)
Field of view	Adjustable from 0.5 to 5.0 mrad
Effective aperture area	0.016 m^2
Predetection filter pass-band width	10 Å
Detector	RCA-7265 PMT (S-20 photocathode)
Frequency response of electronics	30 MHz
Auxiliary Features	
Pointing control	Motor-driven azimuth and elevation; selectable, programmed elevation scanning and firing
Signal conditioning	Automatic range compensation, logarithmic amplification
Recording	Video magnetic disc
Data displays	RHI and A-scope

restricts the number of angular intervals that can reasonably be sampled during horizon-to-horizon scans. For example, a scan from 20 deg elevation above the western horizon to 20 deg elevation above the eastern horizon would require 140 min to complete when using angular intervals of 1 deg, but only 28 min when using angular intervals of 5 deg. Most lidar observations were made at angular steps of 5 deg. During classical, steady-state wave conditions, the effect of time difference across the cross section is not believed to be significant. Figure 2 shows a vertical cross section constructed from lidar data that were obtained when a high-level "standing" wave cloud was observed in the lee of Lone Pine Peak on 18 March 1969. Although 30 minutes were required to complete the lidar scan, the lenticular cloud was observed to remain stationary, with only minor changes in its small-scale billow structure. During the low-level wave conditions that were observed in the lee of Mt. Rose, Nevada, lee waves appeared to be more transient, and wave clouds showed great variability in time. In this case, the cross sections of lidar data represent a time-averaged state of the sky. The effects of time lag on the spatial distribution of lidar echoes in a vertical cross section are minimized when the SRI/APCO Mk VIII lidar is used. This liquid-cooled ruby system transmits a 0.9 joule pulse every 3 seconds. Consequently, a vertical cross section of lidar data collected by scanning from 20° elevation above the western horizon to 20° elevation above the eastern horizon requires 7 minutes when using angular steps of 1 deg, and only 5 minutes when using angular steps of 2 deg. The received atmospheric backscatter signals as a function of range are stored on a magnetic disc recorder and "played back" after each horizon-to-horizon scan in the form of an RHI display of range-corrected, intensity-modulated data. Thus, vertical cross sections of lidar detected atmospheric structure are obtained in near real time without the need for laborious hand-analysis techniques. Figure 3(a) shows a photograph of the Mk VIII

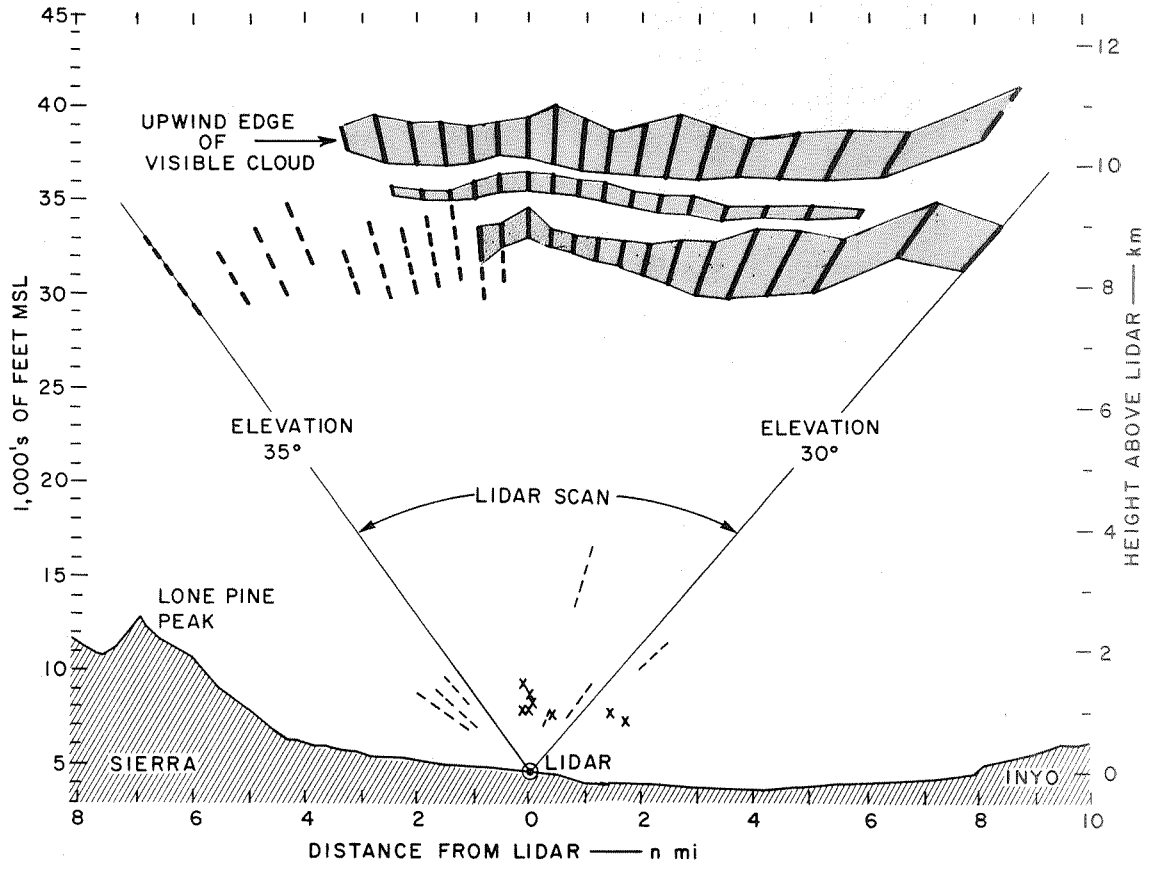

FIGURE 2 VERTICAL CROSS SECTION OF ATMOSPHERIC STRUCTURE CONSTRUCTED FROM LIDAR DATA OBTAINED DURING MODERATE LEE-WAVE DEVELOPMENT NEAR LONE PINE, CALIFORNIA, 18 MARCH 1969, 13:38-14:10 PST. Shading—lenticular cloud; dashed lines—subvisible structure; crosses—dust concentrations.

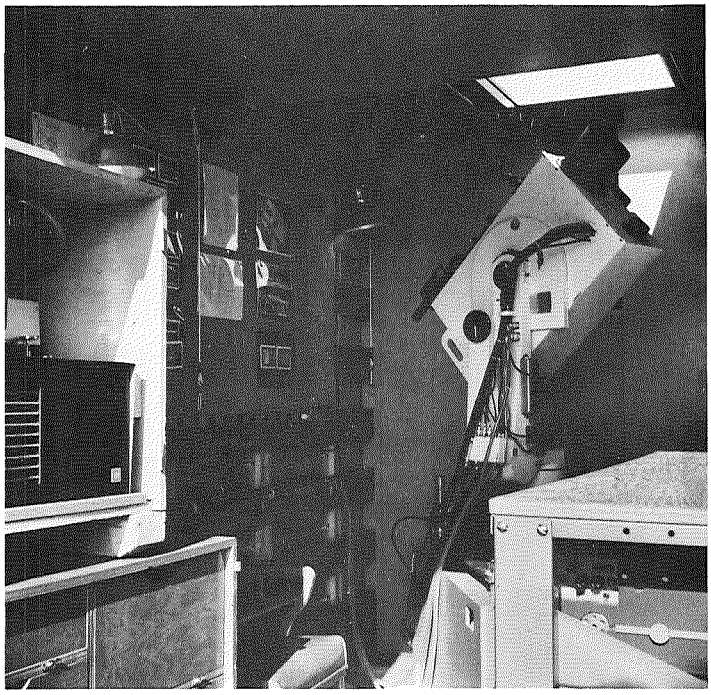

(a) INTERIOR OF LIDAR VAN

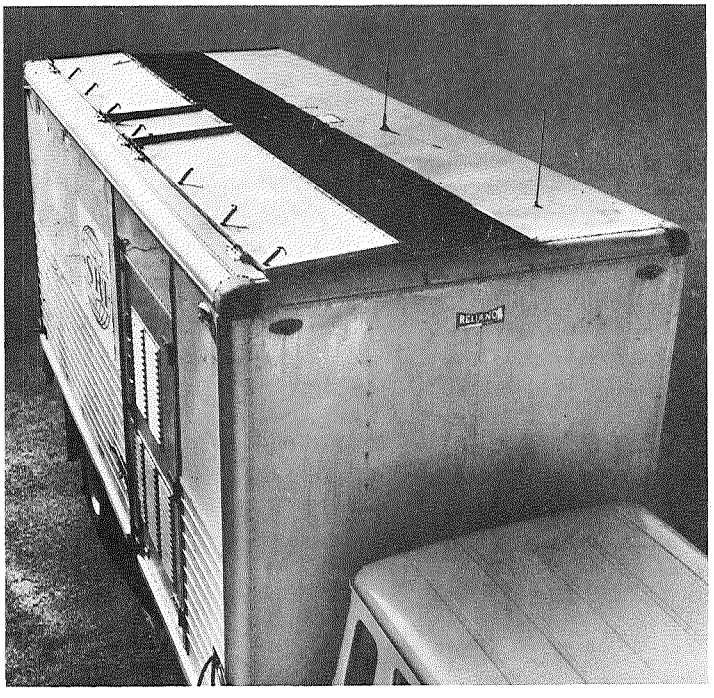

(b) ROOF OF LIDAR VAN OPENED TO ALLOW 140° ANGULAR SCANNING SECTOR

FIGURE 3 MOBILE SRI/APCO Mk VIII LIDAR UNIT USED DURING MOUNTAIN-WAVE OBSERVATION PROGRAM IN THE NORTHERN SIERRA NEVADA

lidar as it is mounted in the van from which it operates. Figure 3(b) shows the roof of the van, which can be opened to allow the lidar to scan over a 140° angular sector within a vertical plane through the zenith. Figure 4 shows an example of a range-corrected, intensity-modulated RHI type presentation composed of all traces from a complete vertical scan. The degree to which the lidar and its data recording and display have been advanced is readily appreciated by a comparison of Figures 2 and 4.

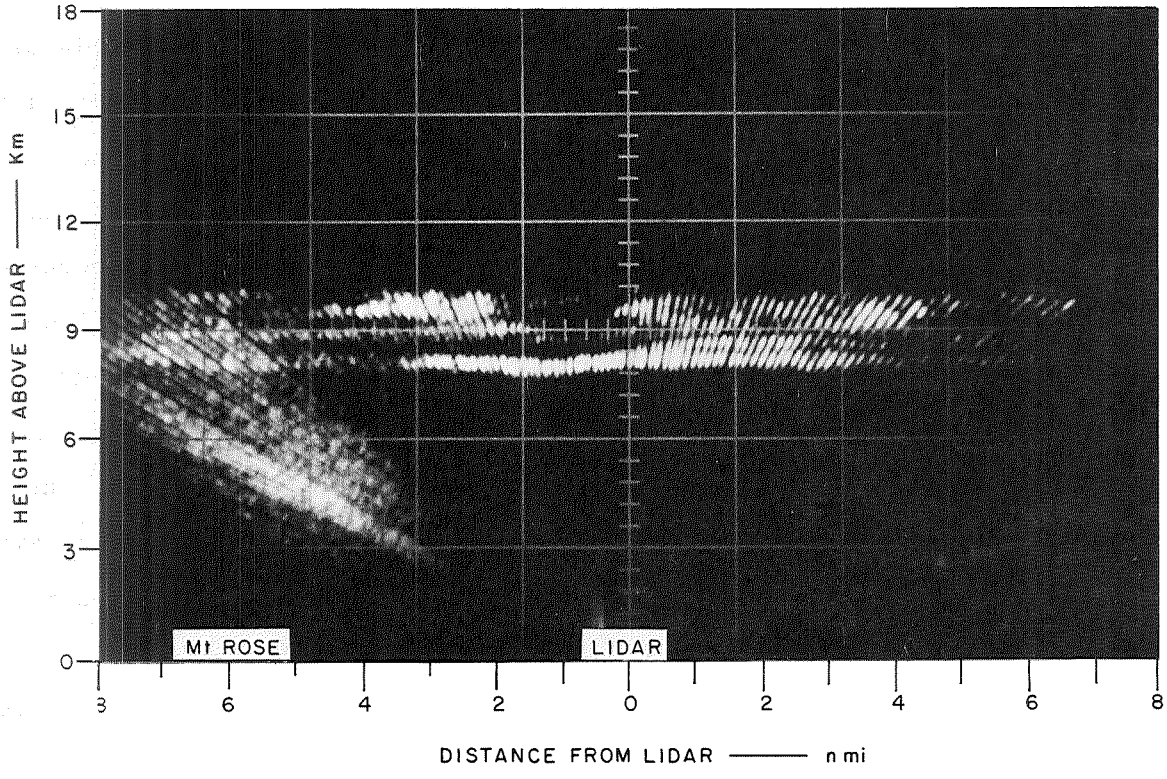

FIGURE 4 CRT DISPLAY OF THE ATMOSPHERIC STRUCTURE DETECTED BY THE Mk VIII LIDAR WHILE SCANNING THROUGH 140° ANGULAR SECTOR AT INTERVALS OF 1°. Mt. Rose, Nevada, 9 February 1971, 13:10-13:17 PST.

IV REVIEW OF LIDAR OBSERVATIONS MADE IN THE SOUTHERN SIERRA NEVADA

During February and March 1967 a series of observations using two pulsed ruby lidars were made near Independence, California (Collis et al., 1968). The observation site was approximately 4500 ft above sea level (MSL) on the lower slopes of the Inyo Mountains on the eastern side of the Owens Valley, due east of the town of Independence. During operation, the lidars were scanned through a E-W vertical plane normal to the mountain ranges, and lidar echoes were recorded at given intervals in elevation angle. Although no strong mountain lee-wave activity occurred, appreciable wave motions were detected, both in what appeared to the eye to be clear air and in air where the particulate matter was sufficiently concentrated as to be visible as clouds. Interruptions in the smooth laminar flow in the clear air were analyzed from the lidar data, and measurements were made of the length, amplitude, and height of wave clouds. With previously existing techniques, only limited observation of these phenomena had been possible. On the basis of the experiment, it was concluded that lidar observations could be of considerable value in studying wave motion, and that lidar observations could possibly be used to infer the presence of turbulence by revealing the breakdown of wave motion or the presence of rotors.

As a consequence of the interesting results of the initial lidar/mountain-wave experiment of 1967, a follow-up observational program was carried out under Contract NAS1-8933 during March and April 1969. The SRI Mk V lidar and GMD-1 rawinsonde equipment were sited on the west side of the Owens Valley at a location 4462 ft MSL, in the lee of Lone Pine Peak (12,944 ft MSL), approximately two miles southwest of the town of Lone Pine. During periods when wave clouds were visually evident,

lidar observations were made in conjunction with rawinsonde ascents and observations by a NASA research aircraft. The general objective of the program was to obtain a better understanding of mechanisms causing hazardous turbulence to aircraft flying over mountain terrain. The particular objective was to establish whether lidar observations (from the ground, as in this program, or subsequently from an aircraft) could be used to delineate the airflow and to detect or anticipate turbulence in mountain waves. Analyses and discussions of the lidar and rawinsonde data collected during the experiment are presented in Scientific Report 1, dated January 1970 (Viezee, 1970). The collected data extend and clarify the observations made at Independence in 1967. For example, of special interest were the observations made at Independence on the afternoon of 19 February 1967 in an easterly flow. To the eye, although patches of altocumulus clouds were apparent over the Inyo Mountains at a height of about 13,000 ft MSL, many of the lidar echoes were recorded under visually clear, blue-sky conditions. When analyzed, these echoes revealed a layer or boundary at the height of the observed altocumulus clouds that appeared to be spatially continuous. The interesting features were the way in which undulations in this subvisible layer occurred and, in particular, the indications of occasional interruptions in this lidar-detected boundary. The interruptions were thought to indicate a breakdown of the wave motion, which, in turn, could be associated with turbulence or with the development of a turbulent rotor region. These interpretations were clarified by the observations made near Lone Pine on 20 March 1969 during westerly flow. The spatial distributions of the lidar echoes from the two series of observations are compared in Figure 5. On 20 March 1969 [Figure 5(b)], the layer of lidar echoes detected in the visually clear sky between the stratus wall to the west of the lidar site and the lenticular cloud to the east is similar to that detected during the

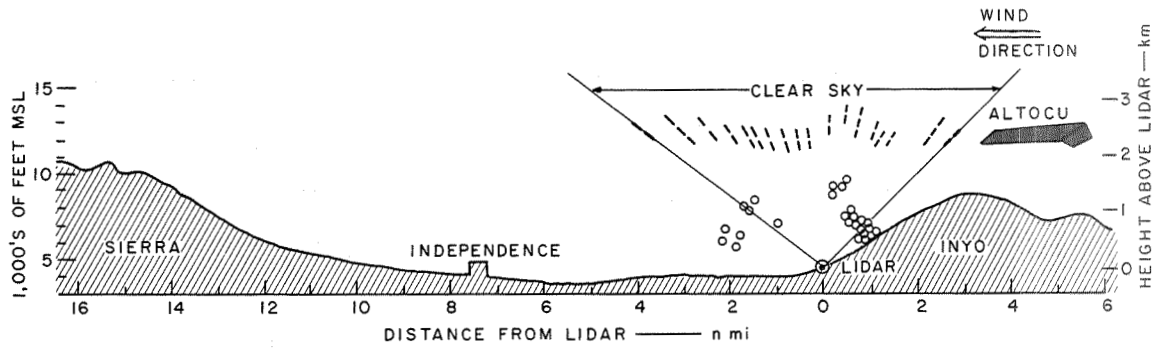

(a) **INDEPENDENCE, CALIFORNIA, 19 February 1967, 13:22-13:43 PST**

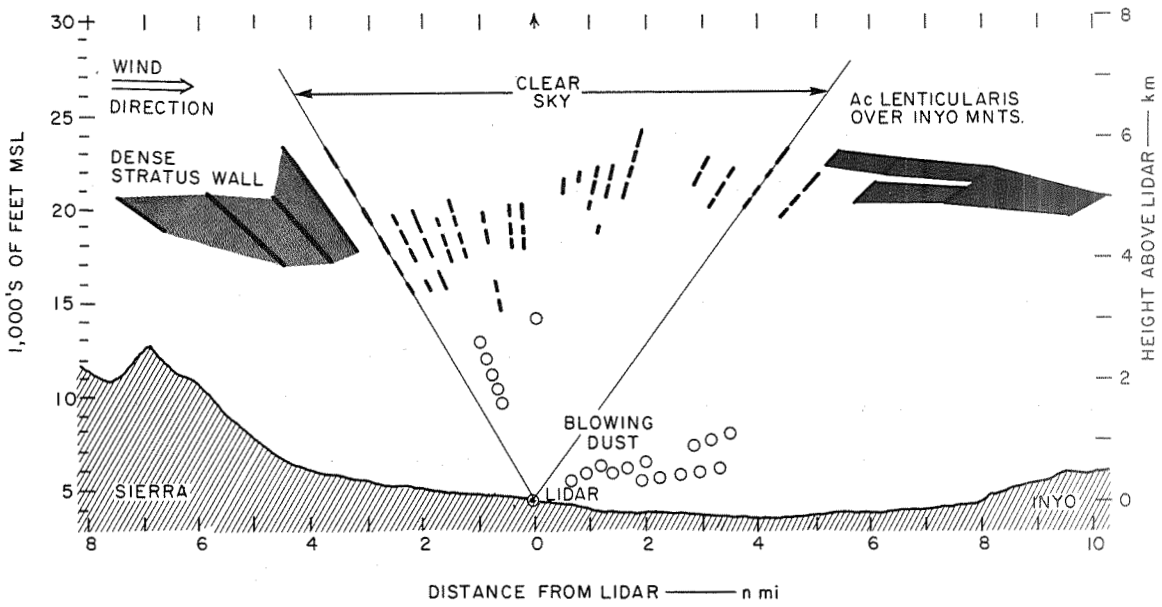

(b) **LONE PINE, CALIFORNIA, 20 MARCH 1969, 15:48-16:25 PST**

FIGURE 5 VERTICAL CROSS SECTIONS OF LIDAR ECHOES SHOWING SIMILARITY IN ATMOSPHERIC STRUCTURE OBSERVED DURING WAVE CONDITIONS OVER OWENS VALLEY ON TWO SEPARATE OCCASIONS. Shading—visible clouds; dashed lines—subvisible structure; open circles—dust.

lidar experiment at Independence on 19 February 1967 [Figure 5(a)]. From visual observations made at the time of lidar-data collection and from the examination of individual lidar traces, it is evident that the "clear air" echoes of 20 March 1969 were connected with thin bands of tenuous cloud that were seen to emerge from the stratus wall. It is believed that they represent concentrations of cloud particles (possibly ice crystals) near the subvisible range that are advected from the stratus wall downwind along the descending air trajectory of the lee region into the ascending trajectory associated with the lenticular cloud over the Inyo Mountains. The "clear air" discontinuities in the lidar data of 19 February 1967 can be interpreted similarly as subvisible concentrations of cloud particles that are advected in the easterly flow downwind from the orographic altocumulus clouds over the Inyo Mountains. The undulating, subvisible layer of cloud particles identifies the early stages of a small-amplitude wave development. When the lee wave intensifies and increases in amplitude, visible lenticular clouds appear in the lee region at the level of this layer as shown by the lenticular cloud in Figure 5(b). The easterly lee wave observed on 19 February 1967 never developed to the extent that pronounced lenticular clouds became visible. The development of a lower turbulence zone is heralded by the appearance of echo clusters (indicated by open circles in the analyses of Figure 5) below the level of the developing wave motion. These clusters arise from dust and variable dust concentrations in the boundary layer. As the rotor region intensifies, cumuliform rotor clouds appear. These clouds develop along the upper boundary of the Turbulent Boundary Layer, which can be easily identified by the sharp decrease in backscatter in the lidar data as shown in Figure 6. Figure 7 illustrates the atmospheric structure analyzed from lidar backscatter signals recorded on 20 March 1969 at a time period after that of Figure 5(b). Noteworthy is the location of the rotor clouds

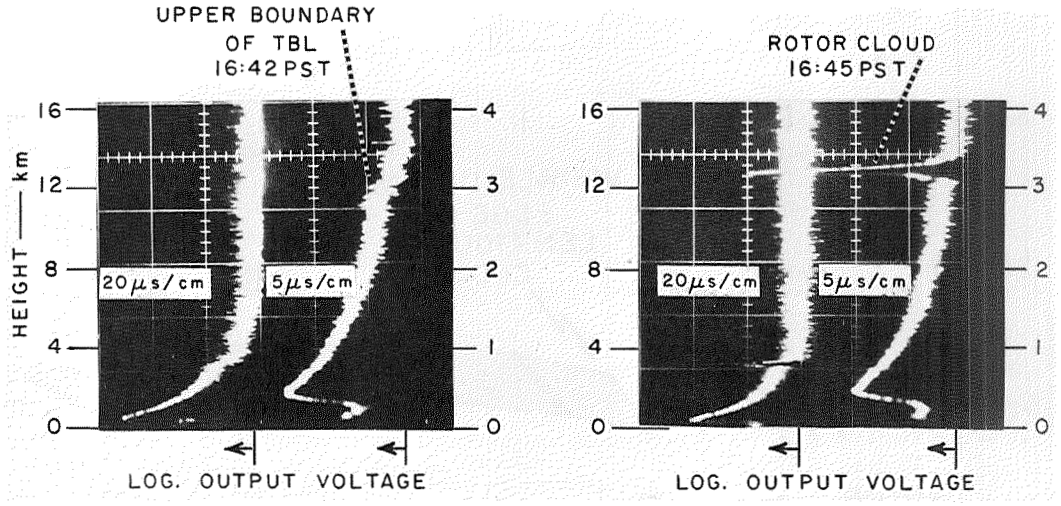

(a) DUAL-BEAM OSCILLOSCOPE DISPLAYS SHOWING THE UPPER BOUNDARY OF THE TURBULENT BOUNDARY LAYER AND THE ROTOR CLOUDS AS IDENTIFIED BY LIDAR

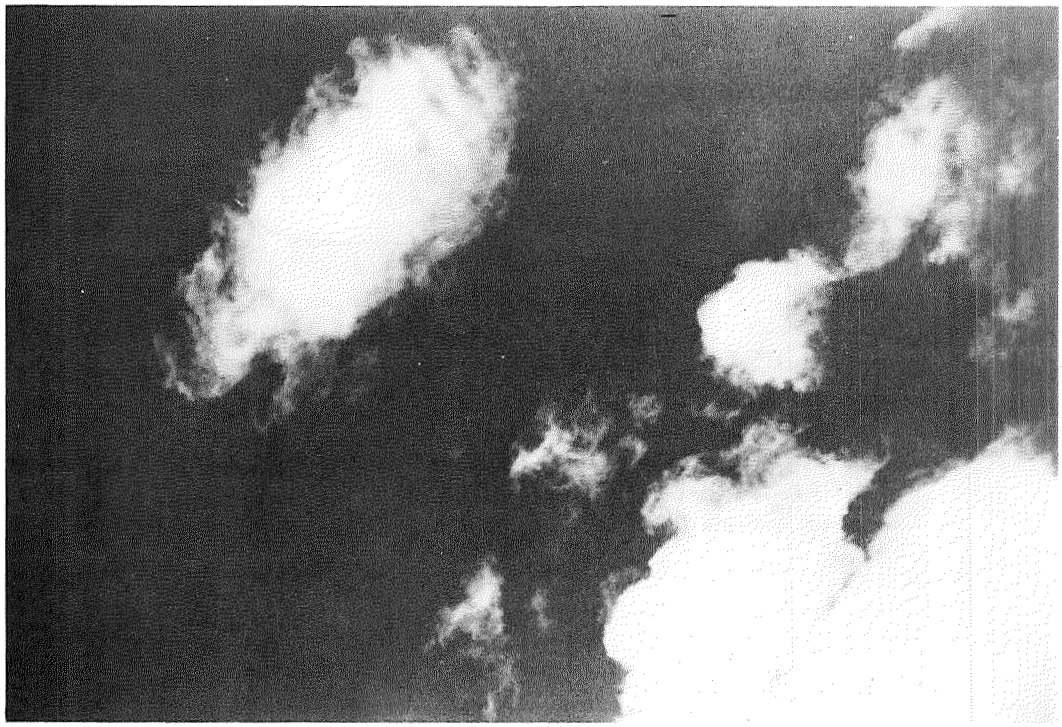

(b) PHOTOGRAPH OF THE LIDAR-DETECTED ROTOR CLOUDS

FIGURE 6 DATA ON TURBULENT BOUNDARY LAYER OBSERVED ON 20 MARCH 1969

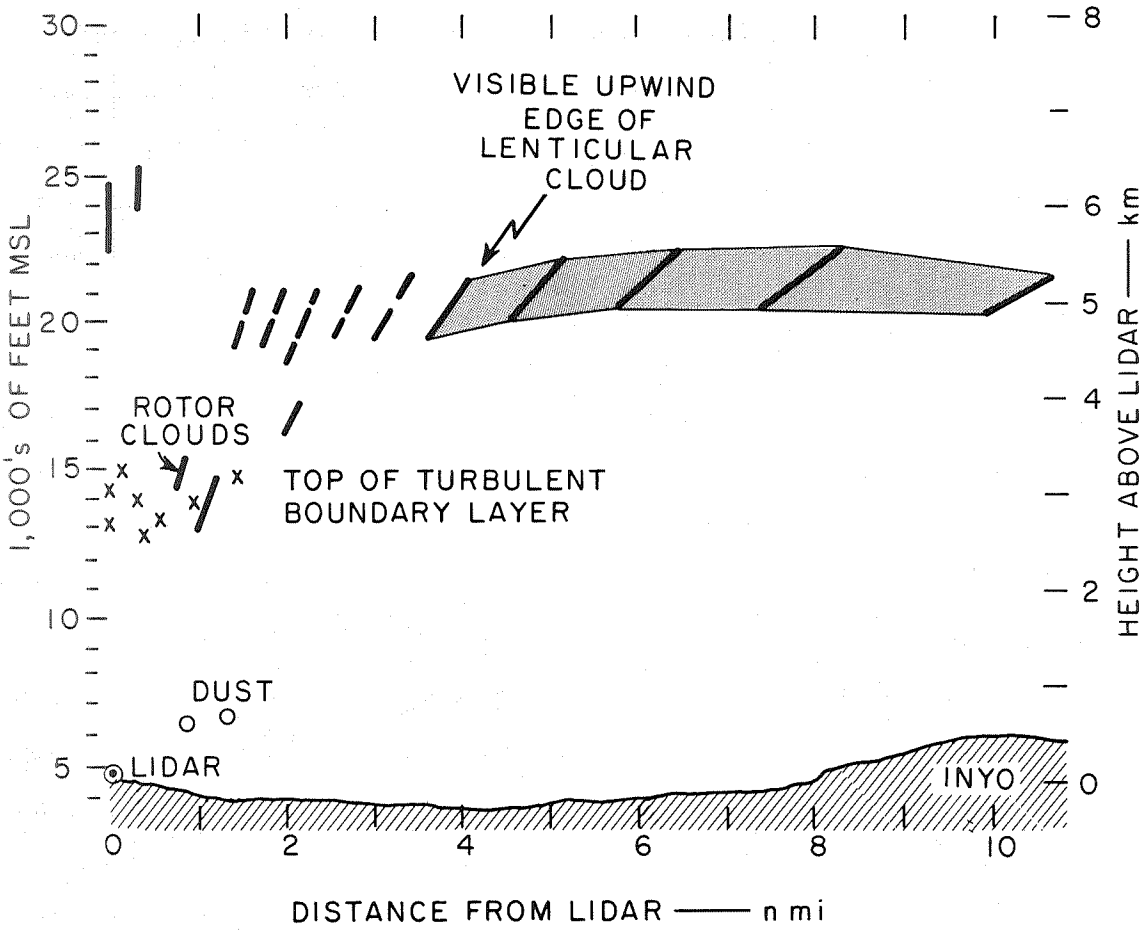

FIGURE 7 VISIBLE (SHADING) AND SUBVISIBLE (DASHED LINES) WAVE CLOUD STRUCTURE OBSERVED BY LIDAR OVER OWENS VALLEY DURING SIERRA-WAVE CONDITIONS ON 20 MARCH 1969, 16:27-16:49 PST. Crosses indicate lidar-detected upper boundary of turbulent boundary layer.

under the upwind edge of the lenticular cloud, a frequently observed feature that differs from that associated with the lee-wave streamline pattern computed by Scorer and Klieforth (1959).

Figure 8 shows rawinsonde data and the wave-cloud structure with the Turbulent Boundary Layer as analyzed from lidar data obtained during a moderate wave development on 18 March 1969. The lidar data were collected during a time period when a T-33 aircraft from the Flight Research Facility of NASA, Edwards explored the area of wave activity. The indicated subjective turbulence reports are typical of what the research aircraft encountered during the 1969 experiment in the southern Sierra Navada: moderate turbulence was always encountered in the Turbulent Boundary Layer under the wave clouds where the lidar detected variable dust concentrations, whereas the tropospheric layer of wave clouds generally presented no more than very light turbulence, which is compatible with the high degree of laminar flow reflected by the lidar-detected wave cloud structure.

The GMD-1 rawinsonde data for the lee-wave case investigated show only expected features such as relatively high wind speeds in the upper troposphere, large vertical shear in the Turbulent Boundary Layer, and a thermally stable layer at the top of the boundary layer. On the basis of these features, the lidar data that were collected are considered representative of a lee wave of moderate intensity. The usefulness of the rawinsonde data in the interpretation of the lidar data was limited by the fact that the radiosonde balloon was released at the lidar site. Consequently, at levels above the rotor region and in the upper troposphere the pertinent rawinsonde data were no longer coincident in space with the lidar data. The rough terrain of the southern Sierra Nevada in the area of operation prevented a launch upwind from the lidar site.

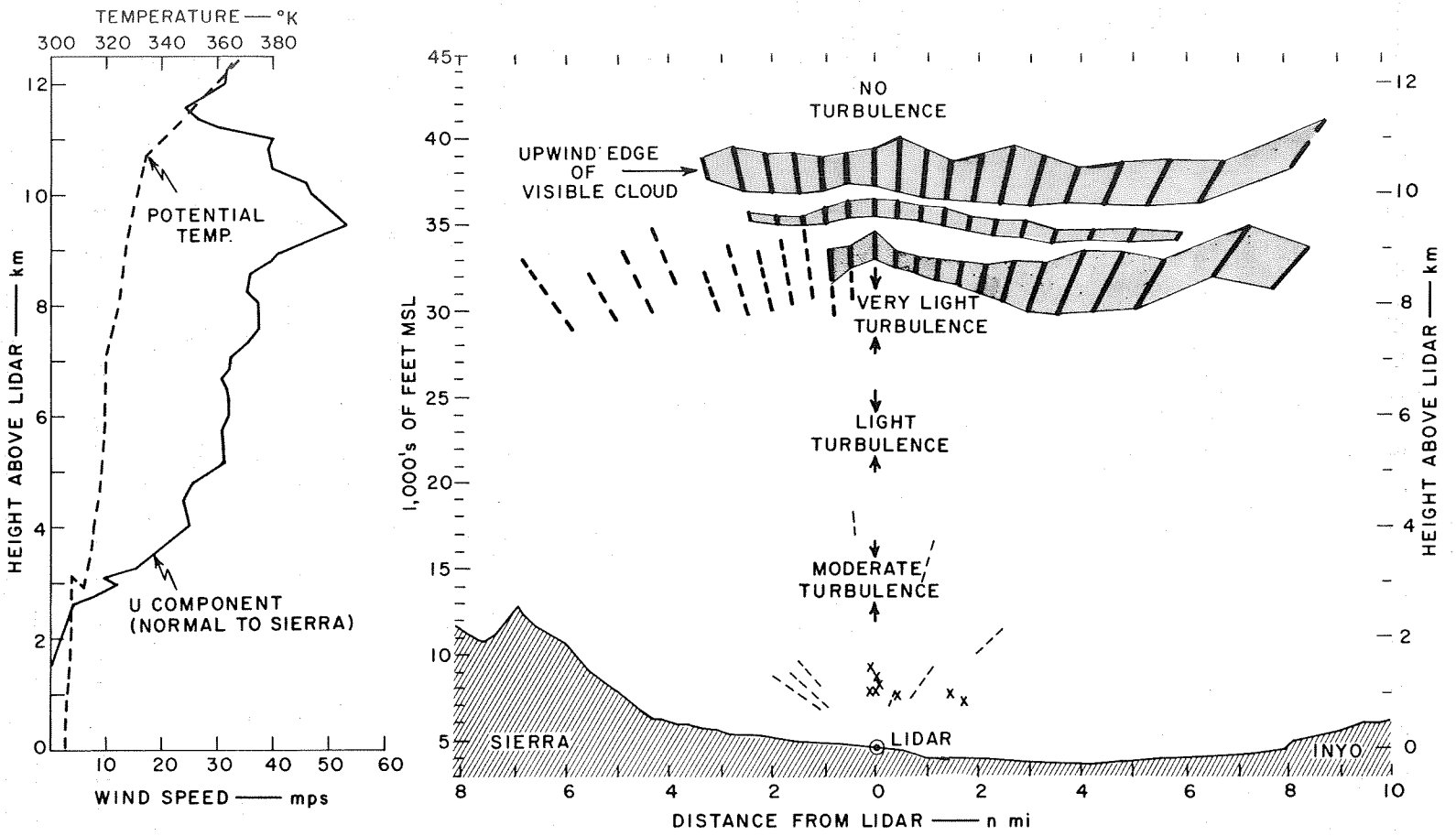

FIGURE 8 RAWINSONDE DATA (14:55 PST) AND WAVE CLOUDS WITH BOUNDARY LAYER ANALYZED FROM LIDAR DATA (13:38-14:10 PST) DURING SIERRA-WAVE CONDITIONS NEAR LONE PINE, CALIFORNIA, ON 18 MARCH 1969. Turbulence reports by NASA Research Aircraft.

V PRESENTATION AND INTERPRETATION OF OBSERVATIONS MADE IN THE NORTHERN SIERRA NEVADA

A. General

Since the wave situations encountered in the southern Sierra Nevada during March and April 1969 did not exceed moderate intensity, it was decided to make additional lidar/mountain-wave observations in the lee of Mt. Rose, Nevada, during the spring of 1970. Under the assumption that the chances of a high-velocity jet stream and subsequently a strong lee wave, would be greater in the northern Sierra Nevada, the lidar equipment and a supporting radiosonde unit* were moved to Reno, Nevada, on 10 March 1970. The road development in this area makes it possible to operate the rawinsonde unit at a site upwind from the location of the lidar. The 16-foot covered van housing the Mk VII ruby lidar and its data-recording equipment was parked on a site 6 miles ENE of Mt. Rose (10,778 ft MSL) and 8 miles SW of Reno. The use of the site (elevation 5,640 ft MSL) was granted to SRI by the University of Nevada. During strong westerly or southwesterly airflow the lidar is located under the primary crest of the Mt. Rose lee wave. The rawinsonde unit was placed at the Truckee-Tahoe Airport, 18 miles WSW of the lidar site. Thus, when the mountain lee wave develops under conditions of westerly winds, the radiosonde balloon is released upwind from the lidar. In Figure 9, terrain profiles of the lee slope in the vertical plane perpendicular to the mountain crest and the location of the lidar with respect to the mountain crest are compared for the southern and northern Sierra Nevada experiments. Although the lee slopes are comparable, differences between the terrain profiles to the west and

*The radiosonde unit used was a rental unit (Model RD-65 Rawinsonde Receiver and Recorder) made by Weather Measure Corporation, Sacramento, California.

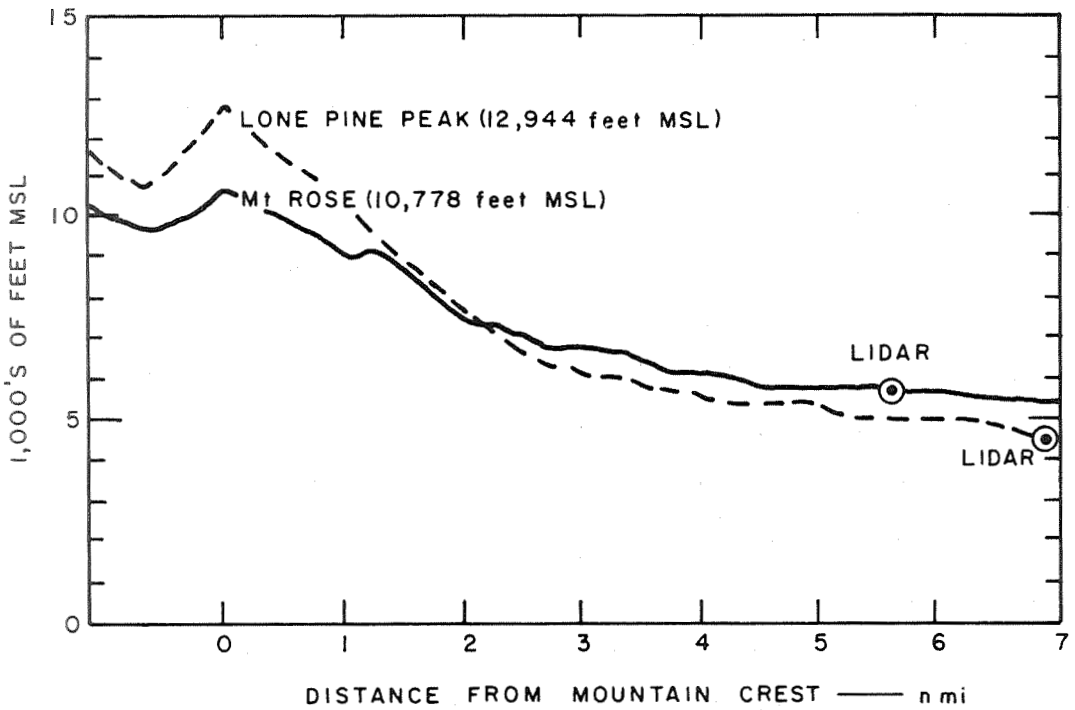

FIGURE 9 COMPARISON BETWEEN LEE-SLOPE PROFILES IN THE VERTICAL PLANE OF LIDAR SCANNING FOR THE OBSERVATION SITES USED IN THE SOUTHERN AND NORTHERN SIERRA NEVADA

northwest of Lone Pine Peak and Mt. Rose introduce significant differences in the configuration of the respective lee waves. During strong westerly or southwesterly flow, the lee wave over the Owens Valley is often a high-level wave resembling the classical configuration described by Holmboe and Klieforth (1957). However, under similar flow conditions the wave in the lee of Mt. Rose is a low-level wave that includes the effects of wave motions generated by several mountain ridges and peaks (7,800 to 9,200 ft MSL) that are located upwind.

Figure 10 shows a photograph of the mountain profile and the location of the lidar van looking west toward Mt. Rose.

On 11 March 1970, lidar and rawinsonde equipment was unpacked, assembled, and calibrated. Preparations were completed to make a series of exploratory observations to check the proper operation of all lidar and rawinsonde equipment components and to familiarize SRI personnel with the position and cloud forms of the Mt. Rose lee wave.

B. Observations of 12 March 1970

On 12 March 1970, lidar observations were collected from 15:00 to 19:30 PST. During this time period, lenticular clouds indicated the presence of a lee wave of light to moderate intensity. Figures 11 and 12 show vertical cross sections of the lidar-observed atmospheric structure during two successive time periods. Examples of the recorded lidar backscatter signals are included in each case. The lidar was fired at intervals in elevation angle selected in such a way as to obtain equal horizontal spacing between the successive lines of sight (and subsequently between the recorded backscatter signals) of about 1600 ft at 25,000 ft MSL.

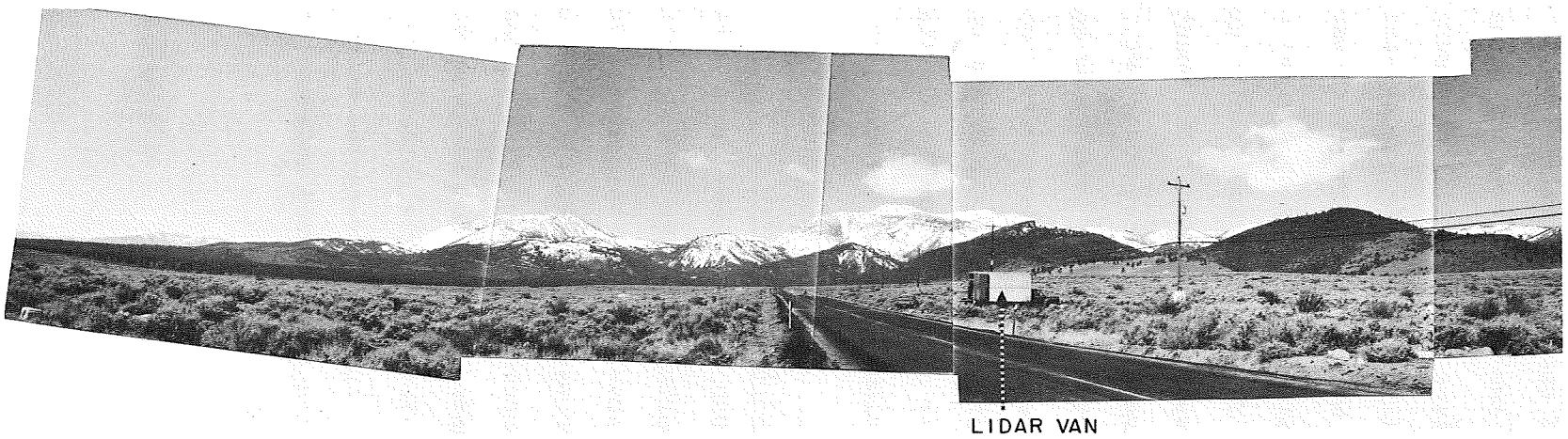

FIGURE 10 LOCATION OF LIDAR VAN IN THE LEE OF THE NORTHERN SIERRA NEVADA.
Viewing west toward Mt. Rose.

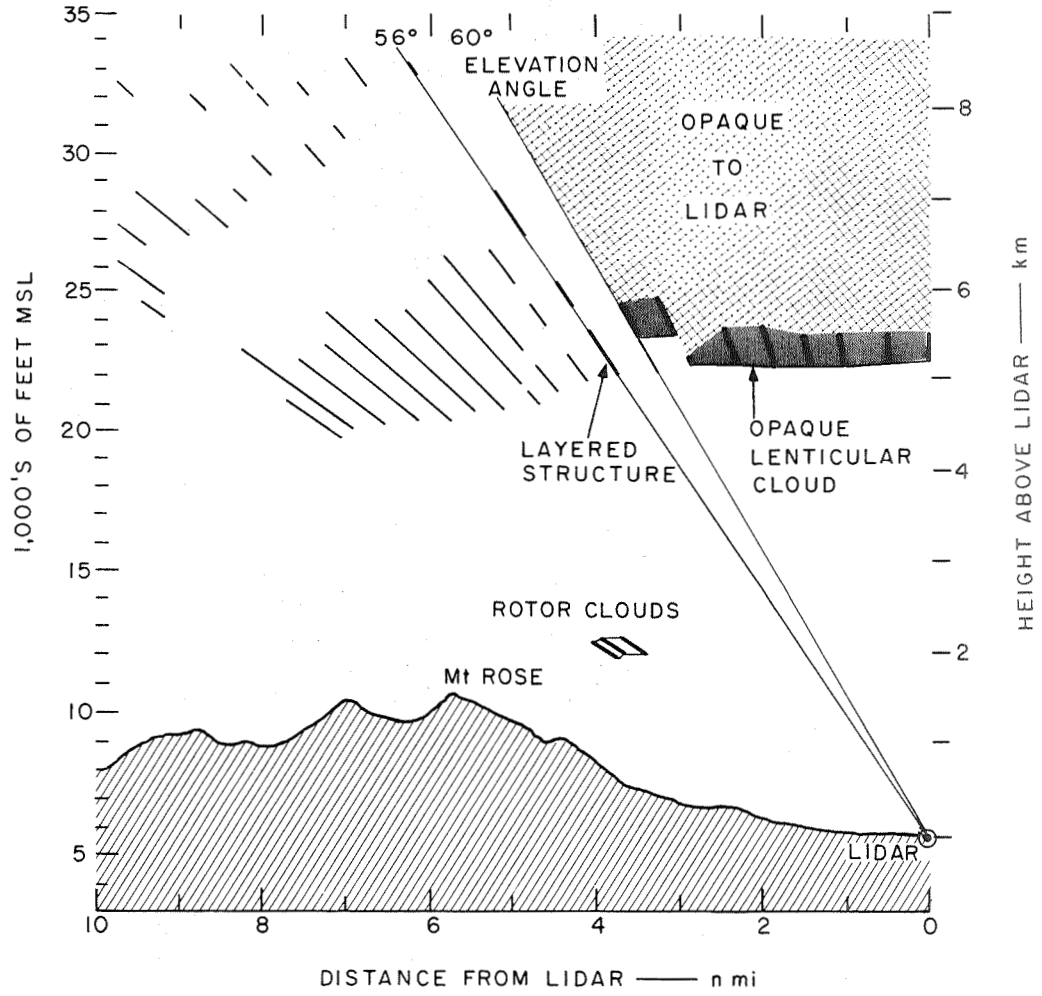

(a) **VERTICAL CROSS SECTION OF WAVE CLOUD STRUCTURE ANALYZED FROM LIDAR DATA OBTAINED BY ANGULAR SCANNING IN A VERTICAL PLANE.** Dark shading identifies opaque lenticular cloud.

FIGURE 11 LIDAR DATA OF MOUNTAIN WAVE RECORDED IN THE LEE OF MT. ROSE, NEVADA, ON 12 MARCH 1970, 18:16-18:45 PST

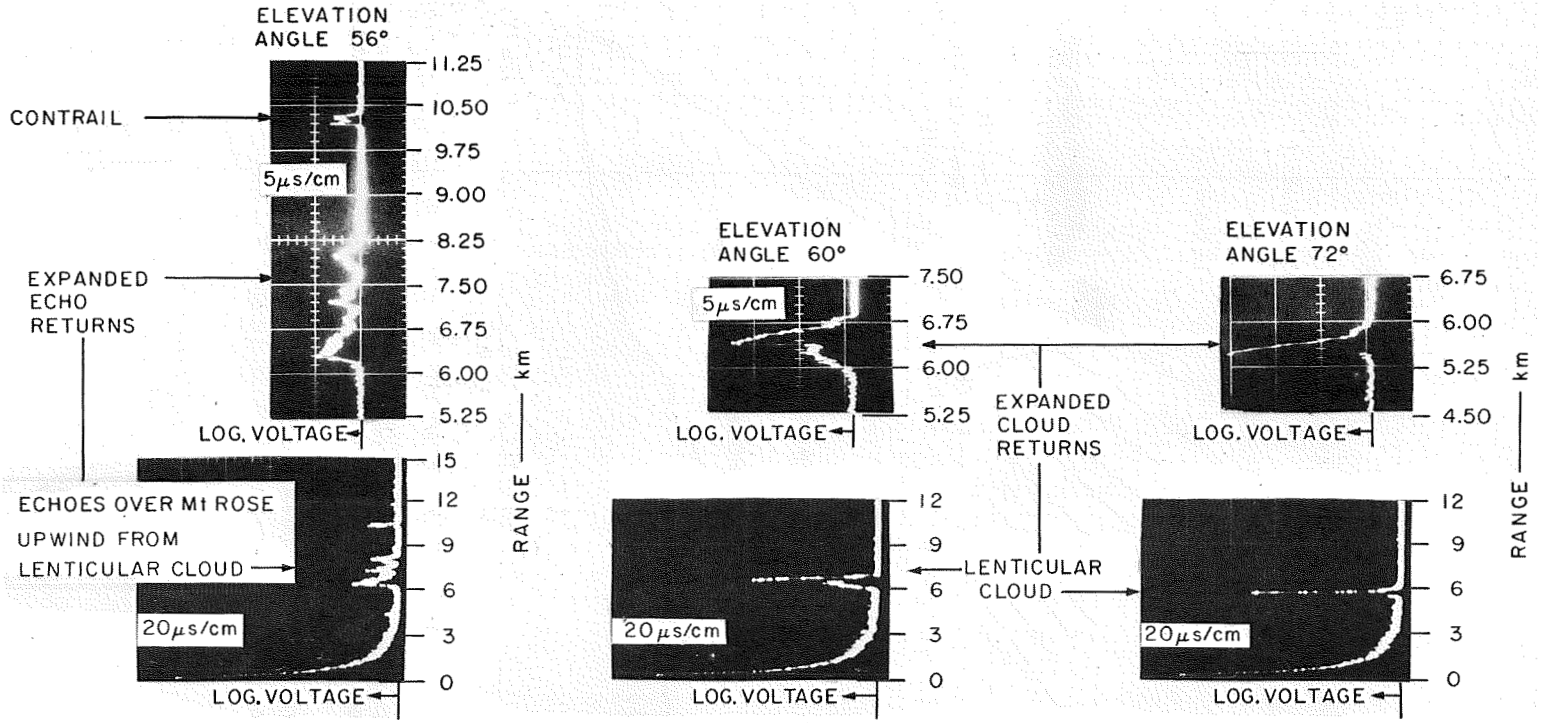

(b) EXAMPLES OF LIDAR BACKSCATTER SIGNALS RECORDED FROM OPAQUE LENTICULAR CLOUD AT 60° AND 72° ELEVATION, AND FROM MULTIPLE-LAYERED TRANSPARENT CLOUD AT 56° ELEVATION

FIGURE 11 LIDAR DATA OF MOUNTAIN WAVE RECORDED IN THE LEE OF MT. ROSE, NEVADA, ON 12 MARCH 1970, 18:16-18:45 PST (Concluded)

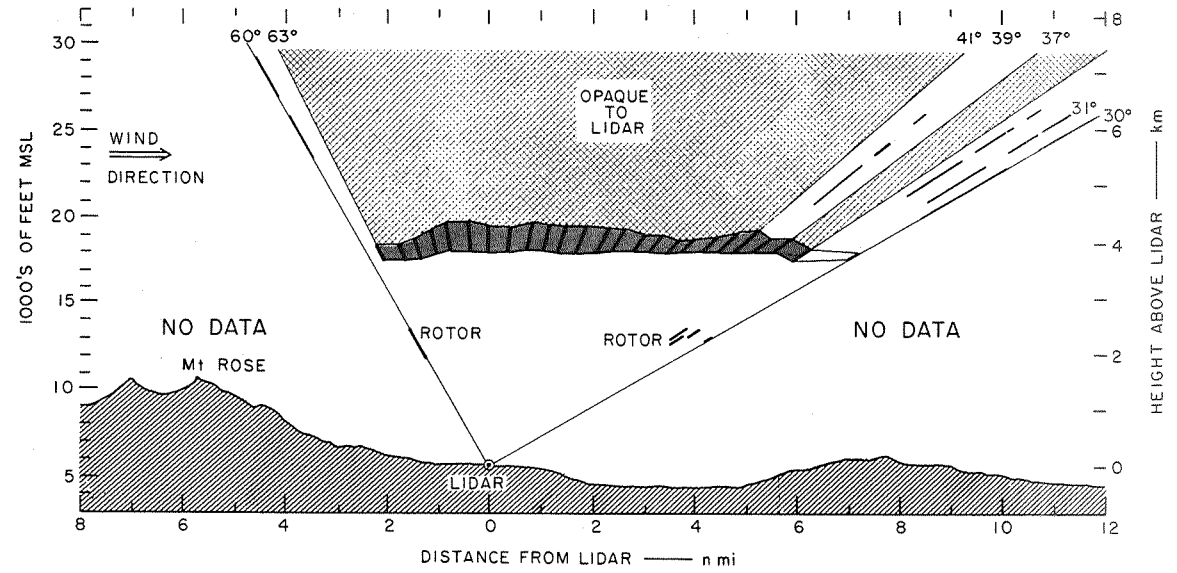

(a) **VERTICAL CROSS SECTION OF WAVE CLOUD STRUCTURE ANALYZED FROM LIDAR DATA. DARK SHADING IDENTIFIES OPAQUE LENTICULAR CLOUD**

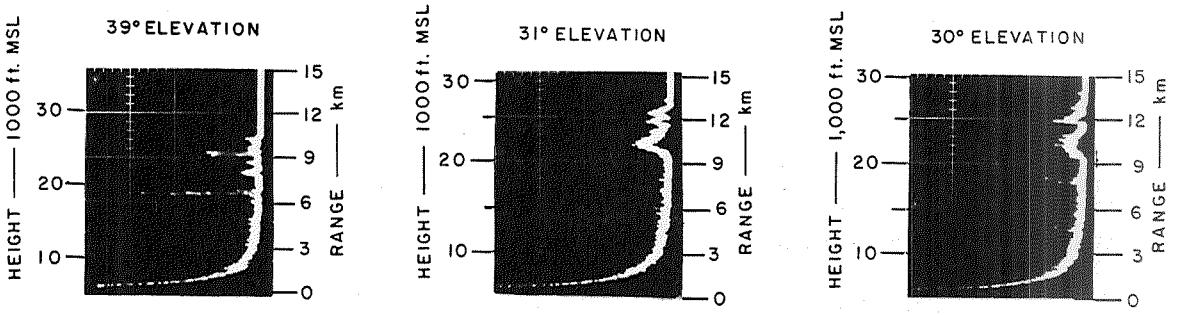

(b) **EXAMPLES OF LIDAR BACKSCATTER SIGNALS RECORDED NEAR DOWNWIND EDGE OF LENTICULAR CLOUD STRUCTURE**

FIGURE 12 LIDAR DATA OF MOUNTAIN WAVE RECORDED IN THE LEE OF MT. ROSE, NEVADA, ON 12 MARCH 1970, 18:47-19:33 PST

Figure 11(a) shows the location of the primary lenticular cloud overhead and to the west of the lidar site. The visible lenticular cloud (indicated by the dark shading) is opaque to the lidar pulse energy and thus shields the upper troposphere above from direct lidar probing. During the time period of observation, the sky beyond the upwind edge of the wave cloud (below 60° elevation angle) was covered with transparent clouds that had the visual characteristics of cirrus. The lidar echoes above 30,000 ft MSL may have been connected with the contrail cirrus that was seen within the field of view of the lidar receiver. The broad layer of backscatter signals recorded over Mt. Rose between 20,000 ft and 25,000 ft MSL represents the tenuous cloud layer in which the lenticular cloud developed. The presence of such a visually transparent layer upwind from a visually opaque lenticular cloud is observed frequently by the lidar (see, for example, Figures 2, 5, and 7). It is likely that the cloud structure of Figure 11(a) portrays the modification of a preexisting layer of tenuous cloud by a standing gravity wave generated partly by topography, upwind from Mt. Rose. The opaque lenticular cloud must correspond to the crest of the lee wave. The layer of transparent cloud upstream from the lenticular cloud shows a distinct multiple-layered structure at a point approximately 1 1/2 mi east of Mt. Rose. Of interest is the optical change from the multiple layers of transparent cloud (at 56° elevation) to the opaque lenticular cloud (at 60° elevation) over a horizontal distance of only 1600 ft. Figure 11(b) shows actual lidar backscatter signals received from the opaque lenticular cloud at 60° and 72° elevation and from the multiple-layered transparent cloud at 56° elevation. From a dual-beam oscilloscope display the lidar signals from the clouds can be examined for detail on an expanded (5μs/cm) scale. The above-mentioned large spatial change in backscatter characteristics from the multiple layers of transparent cloud to the opaque lenticular cloud

over a horizontal distance of only 1600 ft is evident from a comparison between the lidar signal returns of 56° and 60° elevation. The expanded (5μs/cm) traces suggest that the large-amplitude return signal recorded at 60 ° elevation that identified the upwind edge of the lenticular cloud lies within a layer of relatively low return signal similar in character to that recorded at 56° elevation. If, below 25,000 ft MSL, the wave-cloud layer shown in Figure 11(a) consisted of super-cooled water droplets (temperature at that level was approximately -30°C), then the large difference in strength of the lidar backscatter signals suggests that the visible lenticular cloud resulted from a rather explosive growth in drop size and/or drop concentration within a strictly laminar flow pattern.

After the data shown in Figure 11 had been collected, an additional lenticular cloud developed at a lower level. Figure 12(a) shows the spatial extent of the newly formed lenticular cloud from the upwind edge (60° elevation angle) to the downwind edge (30° elevation). Because of rapid extinction of the lidar pulse energy, the atmospheric structure above this lower lenticular cloud (from 63° to 41° elevation) could not be detected. However, near the occasionally transparent edges (60° elevation upwind and < 41° elevation downwind) the lidar data show the presence of higher cloud layers, probably representing those observed earlier and portrayed in Figure 11(a). Figure 12 (b) shows the actual lidar backscatter signals recorded at 39°, 31°, and 30° elevation angle. The presence of a broad multiple-layered cloud structure with relatively low backscatter characteristics at a height between 20,000 ft and 25,000 ft MSL is clearly evident in the data from all three elevation angles. This layer is the same as that detected earlier [see Figure 11(b)]. The two large backscatter signals detected at 39° elevation are characteristic of lidar returns received from dense water clouds. The lower signal represents the thin, transparent downwind edge of the

lenticular cloud shown in Figure 12(a). The upper signal, located near 25,000 ft MSL, and embedded within a broad, multiple-layered cloud structure, represents the downwind edge of the lenticular cloud detected earlier and portrayed in Figure 11(a). The lidar data indicate that the lenticular cloud consisted of larger droplets and/or larger droplet concentration than the layer in which it developed. Although the broad cloud layer persists in the lidar traces at 31° and 30° elevation, the large backscatter signals from the lenticular clouds have either disappeared (at 31° elevation) or show in greatly reduced strength (at 30° elevation), which implies that the cloud elements characteristic of the lenticular clouds are rapidly disappearing, possibly in the downward trajectory of the wave trough. The change in strength of the backscatter signals near the downwind edge of the lenticular clouds shown by the data in Figure 12(b) provides additional evidence that the clouds consisted of water droplets. Ice crystals would not have disappeared as rapidly, especially since the lee wave was judged to be of only light-to-moderate intensity, with no large-amplitude trajectories. The data illustrate the potential of lidar to investigate in detail the structure and optical characteristics of wave clouds. The latter, in turn, reflect the high degree of laminar (nonturbulent) flow in the atmospheric layer of the wave clouds.

C. Observations of 13 March 1970

On 13 March 1970, radiosonde balloons were launched from the Truckee-Tahoe Airport at 10:30 PST and at 13:45 PST; lidar data were collected from 0900 to 1100 PST. No wave clouds were observed during this time period, but an extensive coverage of high clouds was present with areas of rapidly developing and decaying billow clouds. Figure 13 shows the lidar data and the comparative rawinsonde data. The exact position of the radiosonde balloon as it came across the field site after

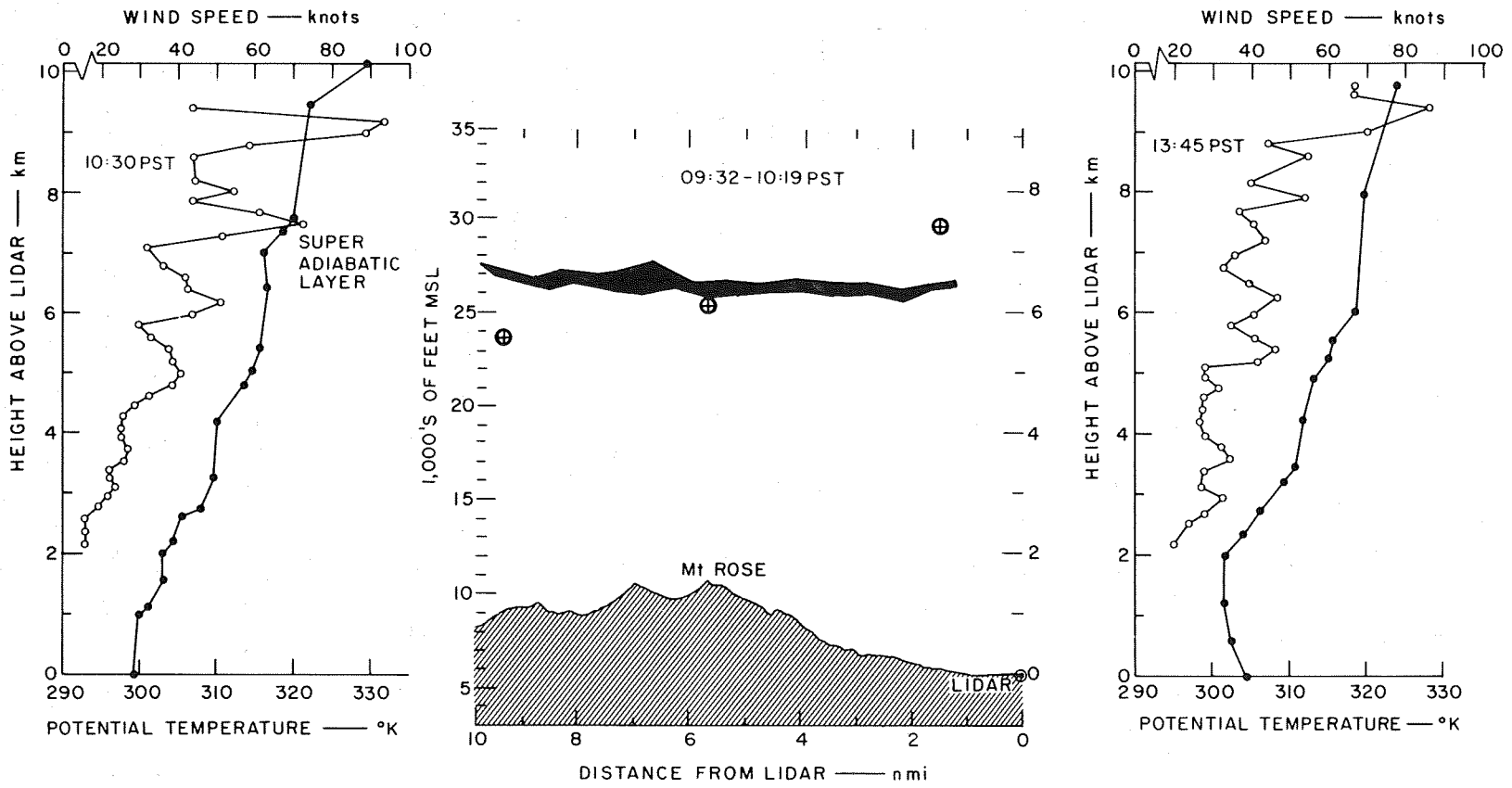

FIGURE 13 RAWINSONDE DATA WITH THE HEIGHT AND SPATIAL EXTENT OF THE LIDAR ECHOES COLLECTED DURING THE OCCURRENCE OF BILLOW CLOUDS IN THE LEE OF MT. ROSE, NEVADA, ON 13 MARCH 1970, 09:32-10:19 PST. Circles indicate position of radiosonde balloon as it crossed the field site after 10:30 PST launch from Truckee-Tahoe Airport.

the 10:30 PST launch is indicated also. The lidar echoes that relate to the observed billow-cloud structure are located in a layer of slightly super-adiabatic lapse rate capped by a temperature inversion. Such a thermal stratification in conjunction with vertical wind shear has been discussed by Sekera (1948) in connection with the development of short gravitational waves of the Helmholtz type. Such waves are recognized as an intermediate stage between laminar flow and fully developed turbulence. The lidar data were obtained by transmitting a single pulse every one to two minutes while changing the elevation angle by 2 to 3 degrees. The observed cloud layer was transparent to the lidar pulse energy, and no particulate matter was detected above or below. Apart from a slight undulation in the layer of lidar echoes over Mt. Rose, no clear-cut identification of billow cloud structure can be made on the basis of the lidar data alone. It is obvious that short-wavelength gravity waves must be investigated with a higher pulse-rate-frequency lidar than was used. Also the ability to rapidly scan at very small intervals in elevation angle ($\leq 1^{\circ}$) seems necessary. It is not known whether or not turbulence was actually present in the layer of billow clouds at the time of lidar probing. It is noteworthy, however, that the 13:45 PST rawinsonde data show a near-adiabatic lapse rate throughout a broad layer centered at the level of the earlier-observed clouds. This layer could have resulted from the effects of turbulent mixing.

D. Observations of 24 April 1970

Because of the development and subsequent persistence of a blocking, high-pressure ridge over the western U.S., no strong mountain waves occurred in the area of operation for a period of 3 to 4 weeks. On 24 April 1970, however, when a strong wave developed, daytime observations by lidar were made during a time period of nearly 7 hours while

three radiosonde balloons were released from the Truckee-Tahoe Airport at intervals of 3 to 4 hours. The intensity of the wave is evaluated on the basis of the so-called Froude number (Long, 1953), defined as

$$Fr = \bar{U}\left[\frac{g\Delta\theta}{\theta} H\right]^{-1/2}$$

where $\bar{U}$ ≡ mean wind component perpendicular to the mountain

$\frac{\Delta\theta}{\theta}$ ≡ static stability throughout the troposphere

H ≡ depth of the troposphere.

Wurtele (1970) computed this theoretical parameter as Fr = 0.20 for the strong mountain wave that dominated the weather situation at the time of the Paradise Airline crash near Lake Tahoe on 1 March 1964. Also, the strong Sierra wave of 16 February 1952, documented by Holmboe and Klieforth (1957), was associated with Fr = 0.24. The values of Fr associated with the Mt. Rose lee wave observed on 24 April 1970 are given in Table 3. The listed values were computed on the basis of the rawinsonde data collected during three separate time periods.

Table 3

Values of the Froude number associated with the Mt. Rose lee wave observed on 24 April 1970

Radiosonde Launch Time (PST)	Froude Number
0950	0.18
1324	0.23
1605	0.27

It is seen that, during the afternoon, Fr exceeded the value of Wurtele's lee wave of 1 March 1964 and of the Bishop wave of 16 February 1952. Thus, the Mt. Rose lee wave of 24 April 1970 can be classified as an intense mountain wave. Figure 14 shows a photograph of the wave cloud system as observed within the field of view of the lidar in the direction of Mt. Rose at an early stage of the wave development.

FIGURE 14 WAVE CLOUD STRUCTURE AS PHOTOGRAPHED DURING EARLY STAGE OF STRONG WAVE DEVELOPMENT IN THE LEE OF MT. ROSE, NEVADA ON 24 APRIL 1970 at 12:03 PST

Figure 15 shows successive positions and altitudes of the radiosonde balloons as they crossed the Mt. Rose mountain ridge 15 to 25 minutes after their release from the Truckee-Tahoe Airport. In the afternoon, during strong southwesterly airflow, the balloons passed within 4 miles north of the lidar site at altitudes close to 30,000 ft MSL. As monitored from the Truckee-Tahoe Airport, the radiosonde balloons were not observed below 10° elevation angle until they had reached 35,000 ft to 40,000 ft MSL. Thus, up to these altitudes, the wind data computed as 2-min averages are considered reliable.

The rawinsonde data collected throughout the day and the wave cloud structure as detected by the lidar are shown in Figure 16. The rawinsonde data are presented in the form of vertical profiles of the (2-min averaged) wind component perpendicular to the mountain range and vertical profiles of potential temperature. The latter give a measure of the all-important static stability. The lidar data were obtained by scanning in a downwind direction starting from the upwind edge of the visible lenticular cloud system. Because of the opacity of the wave clouds, the lidar describes only the spatial distribution of the lower cloud-boundaries and, on occasion, the inclined (upwind) stacking of the wave cloud elements. The lidar and rawinsonde data show the following features of interest.

(1) The rawinsonde data show typical features associated with the development of a lee wave and its intensification with time--i.e., large static stability within a lower tropospheric layer of increasing depth (4000 to 6000 m above the lidar) surmounted by air of lesser stability above; a steady increase with time of the wind speed perpendicular to the mountain range; a pronounced temperature inversion just above the crest of the mountain range at the time of maximum wave development (16:05 PST).

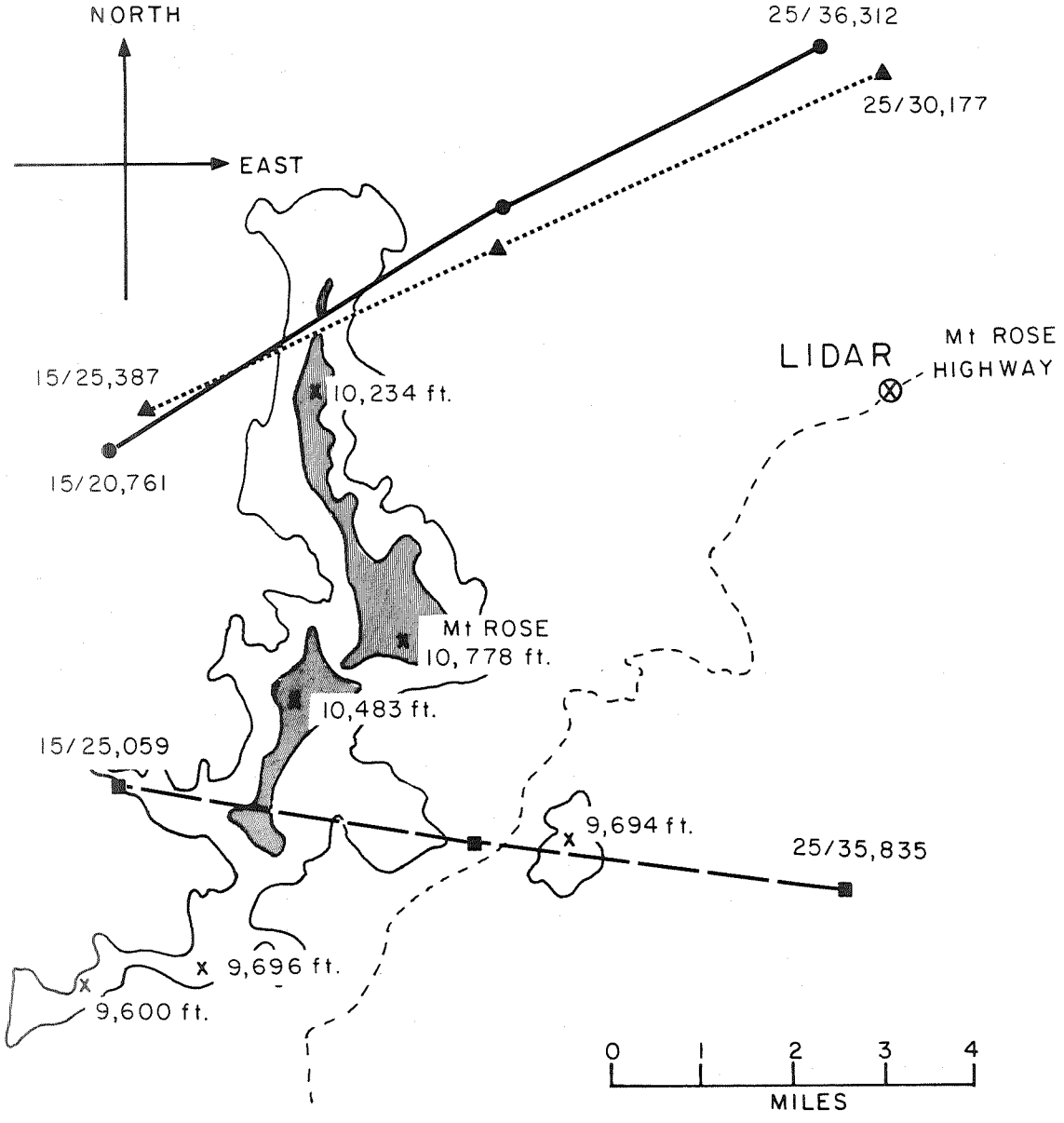

FIGURE 15 SUCCESSIVE POSITIONS AND ALTITUDES OF THE RADIOSONDE BALLOONS AS THEY CROSSED THE MT. ROSE MOUNTAIN RIDGE 15 TO 25 MINUTES AFTER THEIR RELEASE FROM THE TRUCKEE-TAHOE AIRPORT DURING THE STRONG WAVE DEVELOPMENT OBSERVED ON 24 APRIL 1970

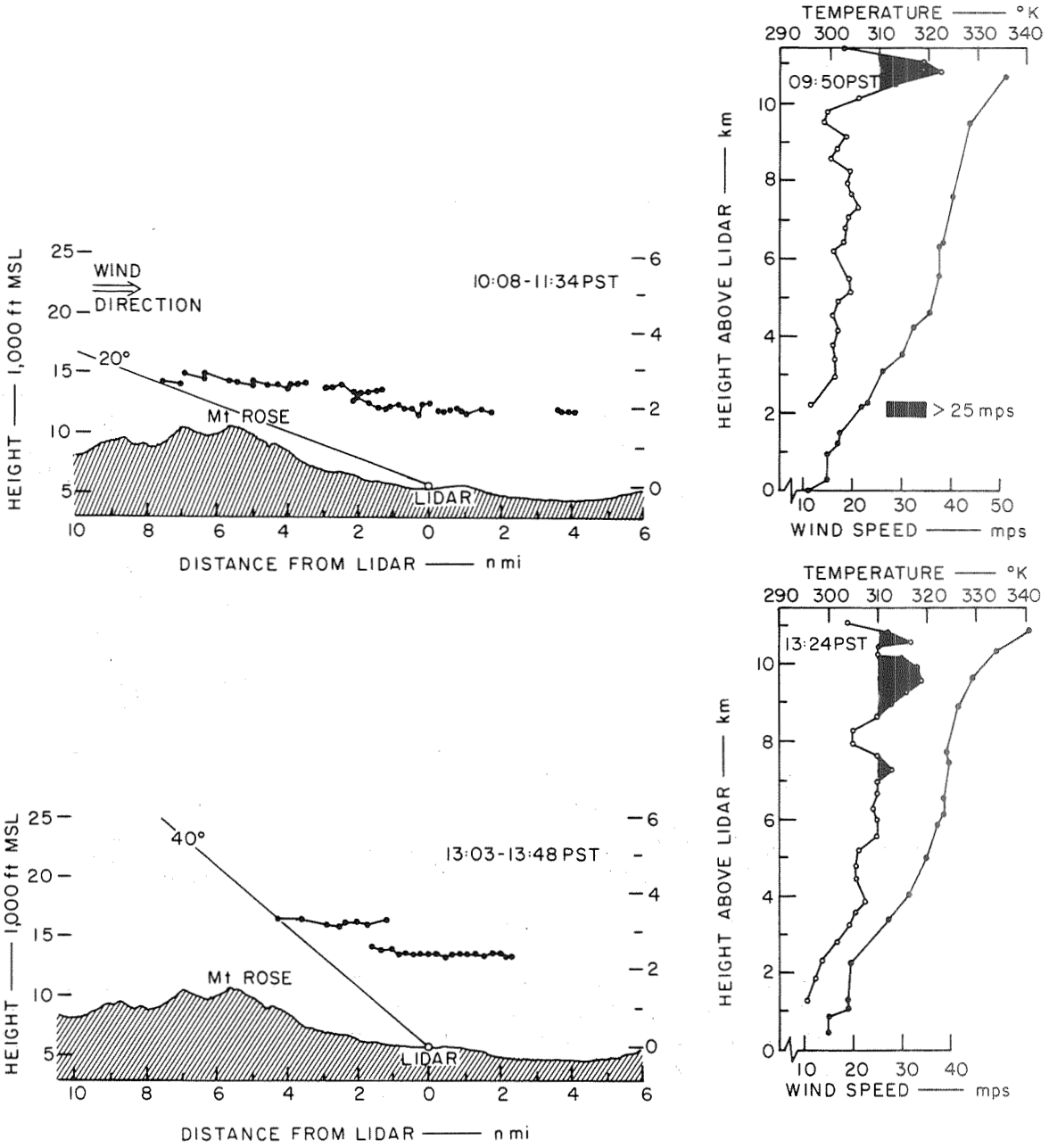

FIGURE 16 COMPARATIVE RAWINSONDE DATA WITH THE WAVE CLOUD STRUCTURE AS DETECTED BY LIDAR FOR FOUR SUCCESSIVE TIME PERIODS DURING THE STRONG WAVE DEVELOPMENT OBSERVED IN THE LEE OF MT. ROSE, NEVADA, ON 24 FEBRUARY 1970

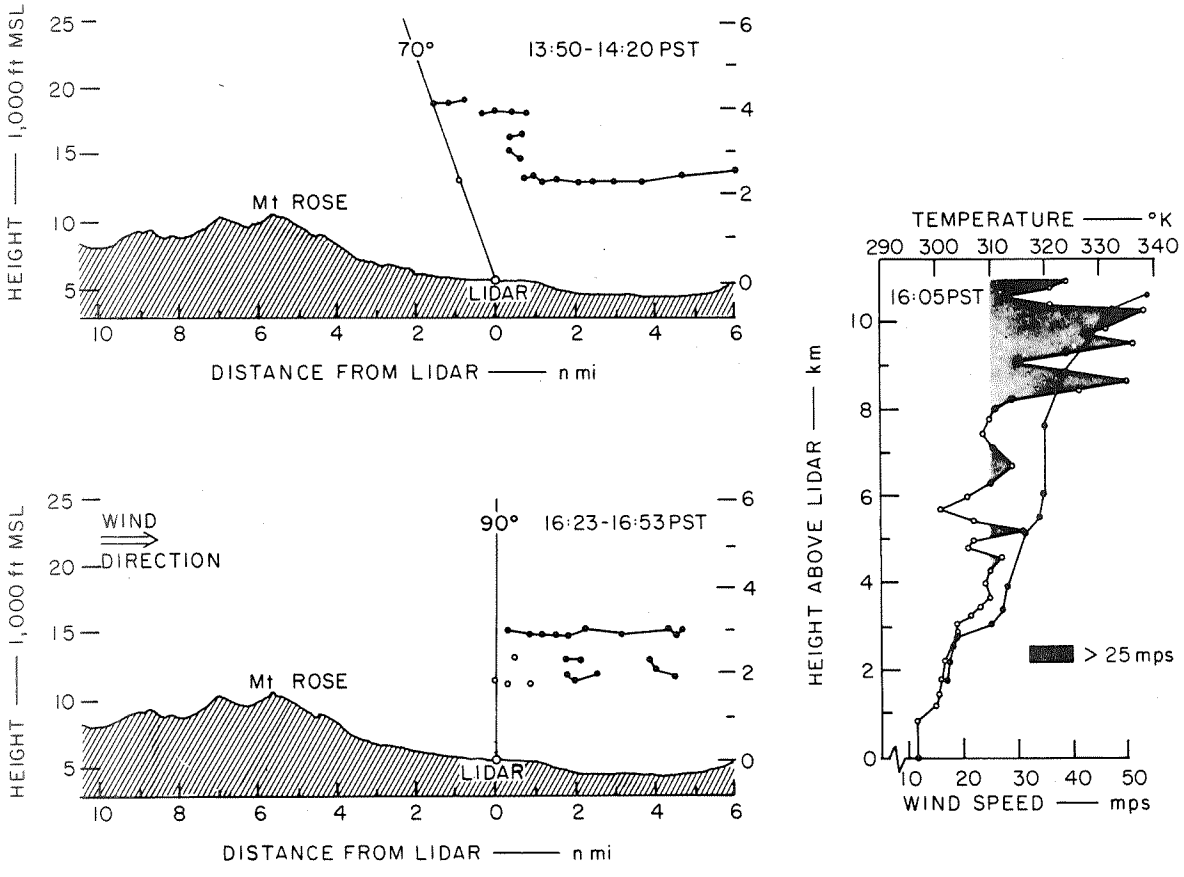

FIGURE 16 COMPARATIVE RAWINSONDE DATA WITH THE WAVE CLOUD STRUCTURE AS DETECTED BY LIDAR FOR FOUR SUCCESSIVE TIME PERIODS DURING THE STRONG WAVE DEVELOPMENT OBSERVED IN THE LEE OF MT. ROSE, NEVADA, ON 24 FEBRUARY 1970 (Concluded)

(2) The lidar data show that the lenticular cloud system propagates in a direction downwind from the mountain crest as the lee wave intensifies. This feature reflects increasing wavelength with increasing wind speed. The elevation angle at which the lidar detected the upwind edge of the wave clouds is indicated in Figure 16 for each time period.

(3) Inclined (upwind) stacking of the wave cloud elements is most pronounced during the early stages of wave intensification (13:03-13:48 PST and 13:50-14:20 PST in Figure 16). During the period of most intense development (16:23-16:53 PST), the wave cloud elements were stacked vertically with little or no upwind inclination. This feature may reflect increasing wave amplitude as well as in-phase arrangement of the waves with height. Figure 17 shows a photograph of the general appearance of the upwind edge of the lenticular-cloud system when the lidar data for the time period 16:23-16:53 PST were collected.

(4) The lower turbulence zone--i.e., the Turbulent Boundary Layer under the wave clouds--as defined by the lidar data extends vertically to a level some 2,000 to 3,000 ft above the mountain crest. Visible rotor clouds, indicated by open circles in the lidar data analysis (13:50-14:20 PST and 16:23-16:53 PST), developed under the upwind edge of the wave cloud system.

(5) As the lee wave intensified, the rawinsonde data show the development of several narrow layers of large vertical wind shear and low static stability in the upper troposphere between 25,000 ft and 40,000 ft MSL.

In Figure 18 the rawinsonde data for the three time periods are analyzed in terms of the vertical variation of the Richardson number,

FIGURE 17 UPWIND EDGE OF LENTICULAR CLOUD SYSTEM OBSERVED IN THE LEE OF MT. ROSE, NEVADA, ON 24 APRIL 1970 AT 16:30 PST

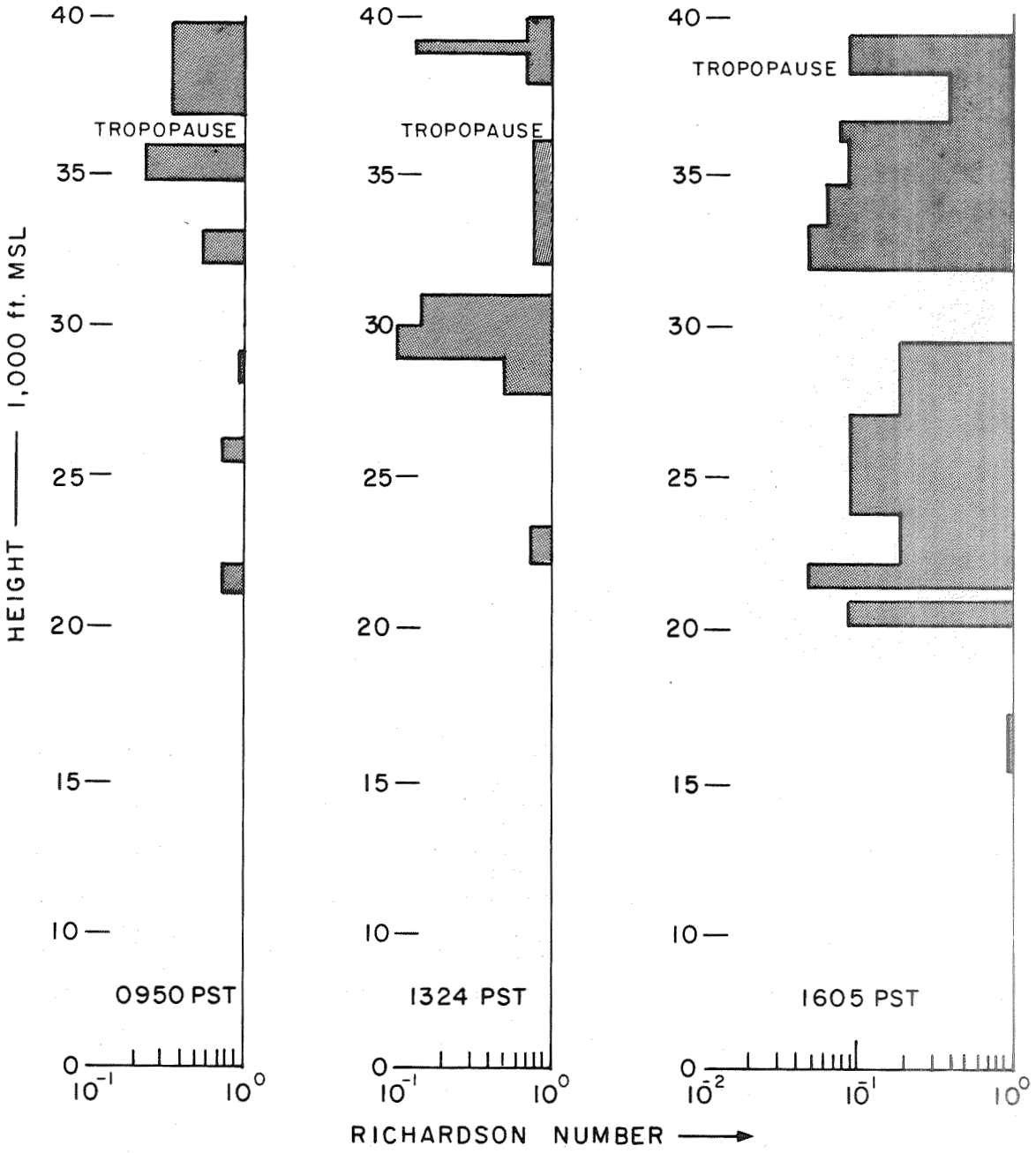

FIGURE 18 VERTICAL VARIATION OF RICHARDSON NUMBER COMPUTED FROM RAWINSONDE DATA AT THREE SUCCESSIVE TIMES DURING THE DEVELOPMENT OF THE STRONG WAVE OBSERVED IN THE LEE OF MT. ROSE, NEVADA, ON 24 APRIL 1970

a stability parameter that approximates the ratio between the forces producing thermal turbulence (static stability) and mechanical turbulence (vertical wind shear). Figure 18 shows that broad layers with Richardson number $\ll 0.25$ developed in the upper troposphere as the wave cloud system moved downwind from the mountain crest. When it is assumed that wave clouds develop within the tropospheric layer of maximum static stability, the vertical profiles of potential temperature suggest that the lenticular clouds did not extend above 20,000 ft to 25,000 ft MSL, since the static stability decreased rapidly above these levels. This implies that the low Richardson numbers developed in the tropospheric layers above the wave clouds. When the Richardson number falls below 0.25, the airflow can become dynamically unstable and can degenerate into turbulent motion. Whether or not aircraft turbulence was or had been associated with these layers of low Richardson number could not be ascertained, since no aircraft flights were reported at that altitude and time.

The data analyses of 24 April 1970 are believed to be significant in that they tend to support the idea that the occurrence or nonoccurrence of mountain-wave turbulence may be inferred from the lidar-detected wave-cloud structure. The absolute values of the computed Richardson numbers cannot be trusted because of possible inaccuracies in the rawinsonde data. There is no doubt, however, that the Richardson numbers decreased significantly as the lee wave increased in intensity. It is also noteworthy that during the last period of observation (16:23-16:53 PST) the visible lenticular-cloud system became disorganized as the lee wave generally showed signs of collapse. Consequently, observations were discontinued after this period.

E. Observations of 6-13 February 1971

A final experiment was carried out in the lee of Mt. Rose, Nevada, during the week of 6-13 February 1971 for the purpose of exploring the applicability of the SRI/APCO Mk VIII lidar system to mountain-wave turbulence observations.

The primary difference in the Mk VIII lidar from its predecessors are:

(1) The Mk VIII is a liquid-cooled system with a stable firing rate of one pulse per 2-3 seconds.

(2) The Mk VIII has the capability of being automatically scanned in equal elevation (or azimuth) increments at selected firing rates.

(3) The transmitter and receiver are coaxial.

(4) The receiver has a disc storage memory with playback features.

(5) A continuous-view two-dimensional intensity-modulated cathode-ray-tube (CRT) presentation in radar RHI or PPI fashion is incorporated.

In order to design the RHI display, it was necessary to incorporate a technique whereby the gain of the receiver is automatically increased as the inverse of the log $1/R^2$ following the laser pulsing. Figures 19 through 26 show a series of CRT displays of the atmospheric structure as observed with the Mk VIII system in the lee of Mt. Rose. Observations were made from the same location as in the earlier experiments (see Figure 10). Each cross section of atmospheric structure is accompanied by a photograph of the cloud cover observed by viewing the zenith from inside the van and an "A"-scope photograph of the lidar echoes as they are stored in the magnetic disc memory in the form of log amplitude (range-corrected) versus range. Each section was obtained in about 7 minutes by selecting a firing rate of 1 pulse per 3 seconds per 1 deg interval

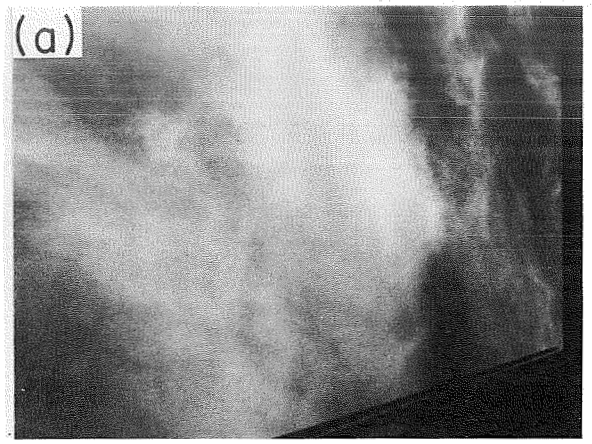

(a) PHOTOGRAPH OF OBSERVED CLOUD COVER

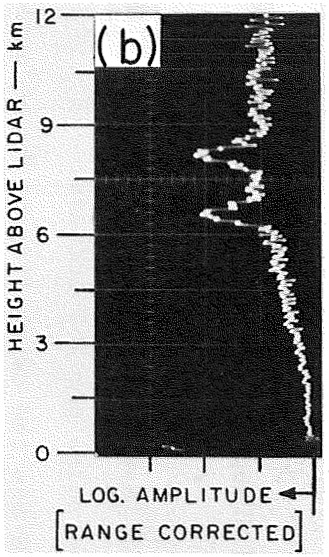

(b) SINGLE LIDAR TRACE (10 μs/cm) OF (RANGE-CORRECTED) LOG AMPLITUDE VERSUS RANGE (90° ELEVATION ANGLE)

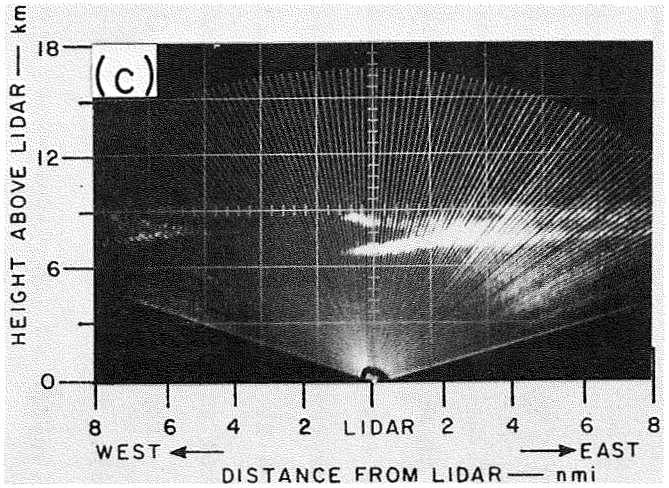

(c) INTENSITY-MODULATED CRT PRESENTATION OF ATMOSPHERIC STRUCTURE IN THE VERTICAL PLANE OF LIDAR SCANNING

FIGURE 19 DATA ON ATMOSPHERIC STRUCTURE OBTAINED BY AUTOMATED LIDAR SYSTEM IN THE LEE OF MT. ROSE, NEVADA, ON 9 FEBRUARY 1971, 09:05-09:12 PST

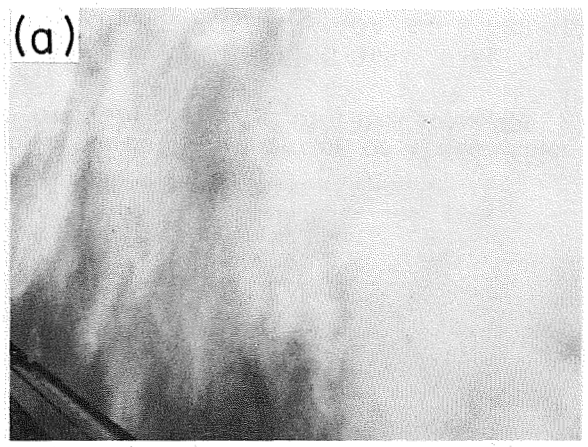

(a) PHOTOGRAPH OF OBSERVED CLOUD COVER

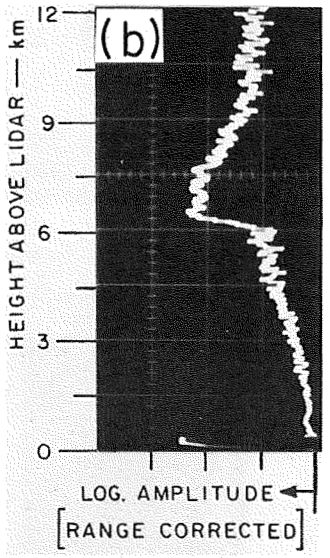

(b) SINGLE LIDAR TRACE (10 μs/cm) OF (RANGE-CORRECTED) LOG AMPLITUDE VERSUS RANGE (90° ELEVATION ANGLE)

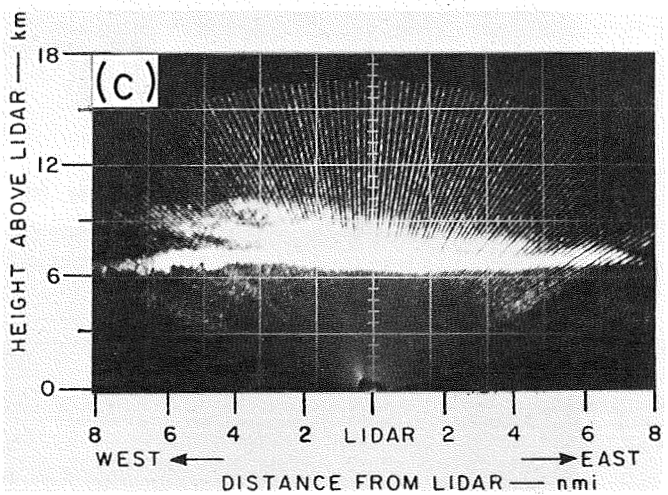

(c) INTENSITY-MODULATED CRT PRESENTATION OF ATMOSPHERIC STRUCTURE IN THE VERTICAL PLANE OF LIDAR SCANNING

FIGURE 20 DATA ON ATMOSPHERIC STRUCTURE OBTAINED BY AUTOMATED LIDAR SYSTEM IN THE LEE OF MT. ROSE, NEVADA, ON 9 FEBRUARY 1971, 11:00-11:07 PST

(a) PHOTOGRAPH OF OBSERVED CLOUD COVER

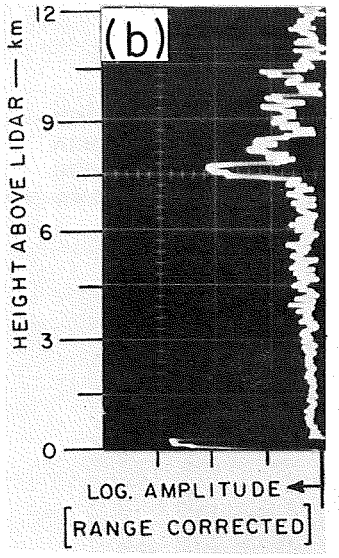

(b) SINGLE LIDAR TRACE (10 μs/cm) OF (RANGE-CORRECTED) LOG AMPLITUDE VERSUS RANGE (90° ELEVATION ANGLE)

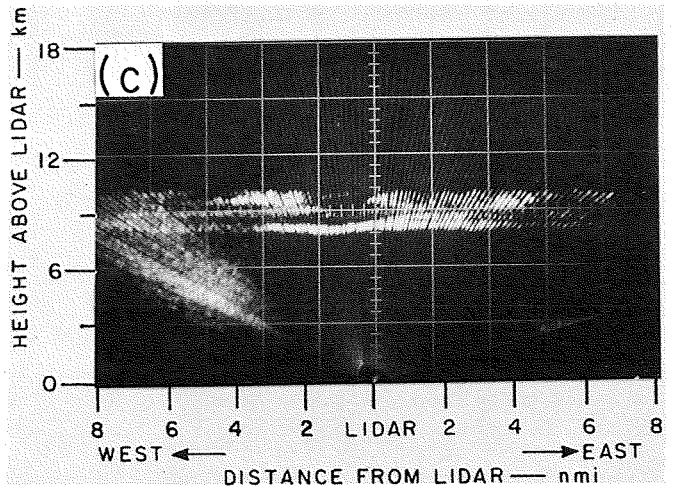

(c) INTENSITY-MODULATED CRT PRESENTATION OF ATMOSPHERIC STRUCTURE IN THE VERTICAL PLANE OF LIDAR SCANNING

FIGURE 21 DATA ON ATMOSPHERIC STRUCTURE OBTAINED BY AUTOMATED LIDAR SYSTEM IN THE LEE OF MT. ROSE, NEVADA, ON 9 FEBRUARY 1971, 13:10-13:17 PST

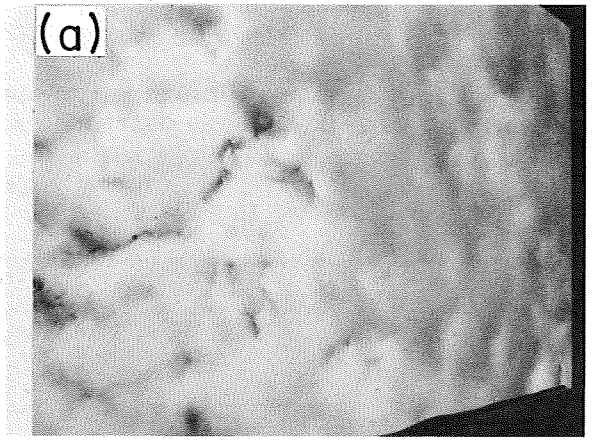

(a) PHOTOGRAPH OF OBSERVED CLOUD COVER

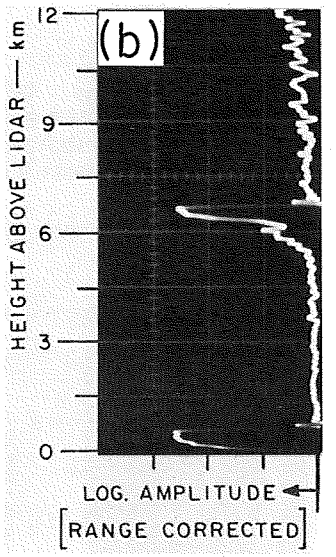

(b) SINGLE LIDAR TRACE (10 μs/cm) OF (RANGE-CORRECTED) LOG AMPLITUDE VERSUS RANGE (90° ELEVATION ANGLE)

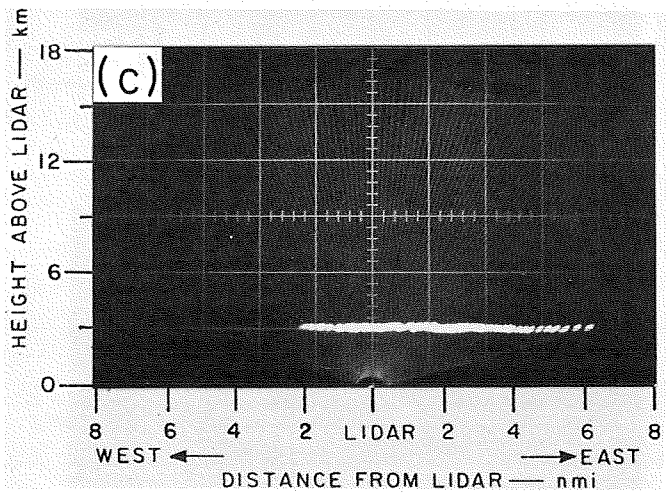

(c) INTENSITY-MODULATED CRT PRESENTATION OF ATMOSPHERIC STRUCTURE IN THE VERTICAL PLANE OF LIDAR SCANNING

FIGURE 22 DATA ON ATMOSPHERIC STRUCTURE OBTAINED BY AUTOMATED LIDAR SYSTEM IN THE LEE OF MT. ROSE, NEVADA, ON 10 FEBRUARY 1971, 09:00-09:07 PST

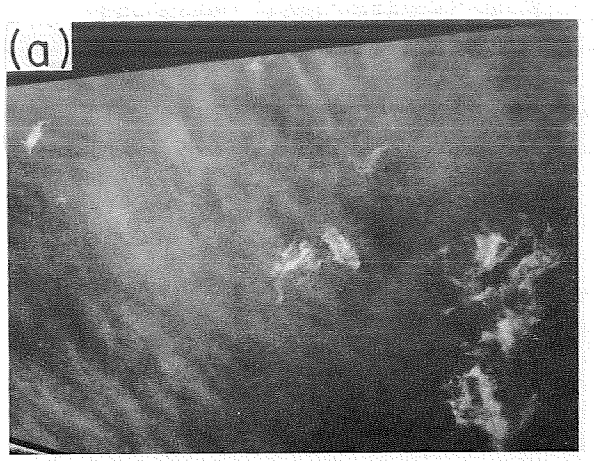

(a) PHOTOGRAPH OF OBSERVED CLOUD COVER

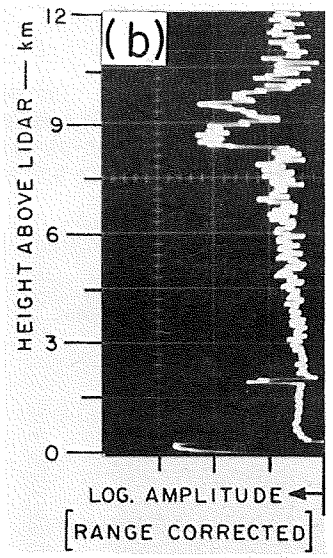

(b) SINGLE LIDAR TRACE (10 μs/cm) OF (RANGE-CORRECTED) LOG AMPLITUDE VERSUS RANGE (90° ELEVATION ANGLE)

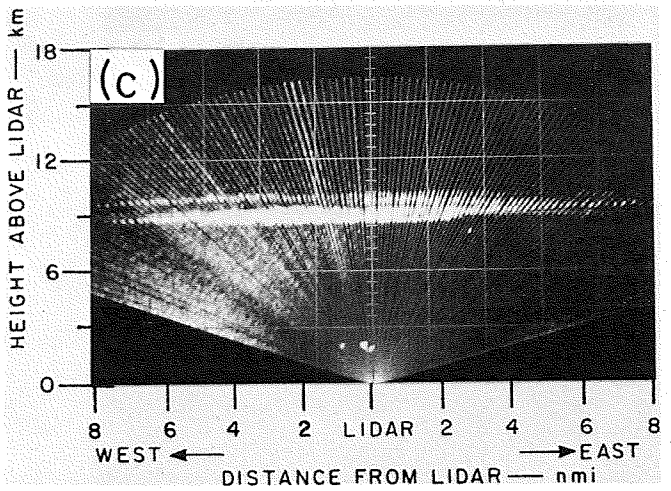

(c) INTENSITY-MODULATED CRT PRESENTATION OF ATMOSPHERIC STRUCTURE IN THE VERTICAL PLANE OF LIDAR SCANNING

FIGURE 23 DATA ON ATMOSPHERIC STRUCTURE OBTAINED BY AUTOMATED LIDAR SYSTEM IN THE LEE OF MT. ROSE, NEVADA, ON 10 FEBRUARY 1971, 14:10-14:17 PST

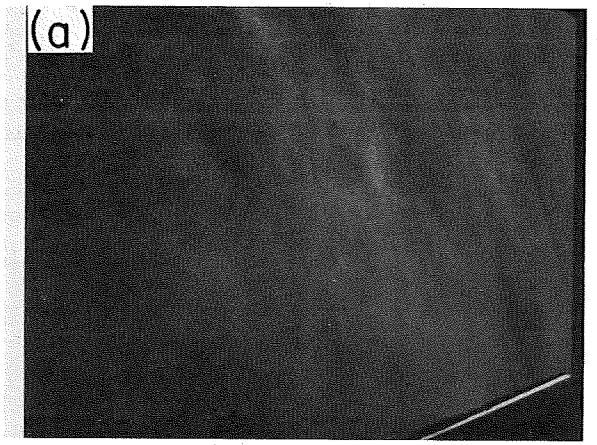

(a) PHOTOGRAPH OF OBSERVED CLOUD COVER

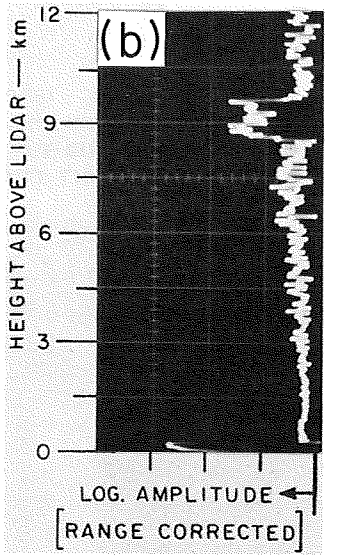

(b) SINGLE LIDAR TRACE (10 μs/cm) OF (RANGE-CORRECTED) LOG AMPLITUDE VERSUS RANGE (90° ELEVATION ANGLE)

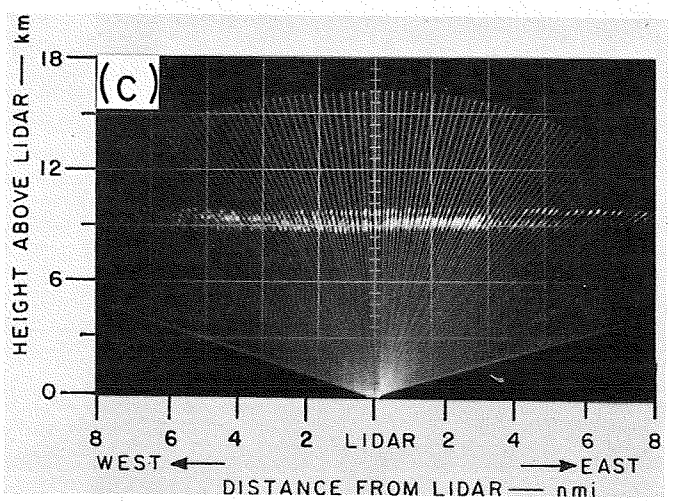

(c) INTENSITY-MODULATED CRT PRESENTATION OF ATMOSPHERIC STRUCTURE IN THE VERTICAL PLANE OF LIDAR SCANNING

FIGURE 24 DATA ON ATMOSPHERIC STRUCTURE OBTAINED BY AUTOMATED LIDAR SYSTEM IN THE LEE OF MT. ROSE, NEVADA, ON 11 FEBRUARY 1971, 10:10-10:17 PST

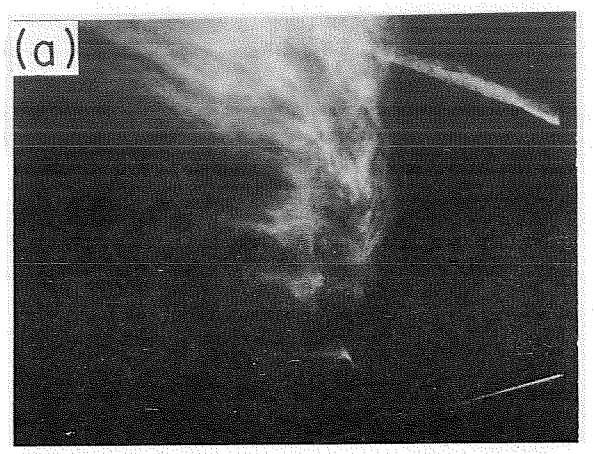

(a) PHOTOGRAPH OF OBSERVED CLOUD COVER

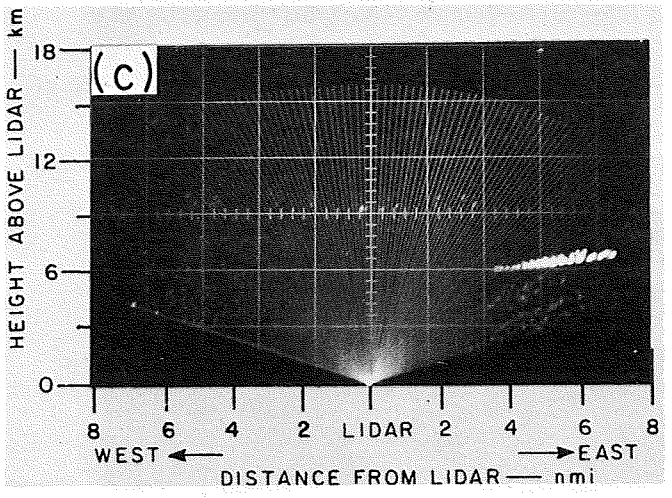

(c) INTENSITY-MODULATED CRT PRESENTATION OF ATMOSPHERIC STRUCTURE IN THE VERTICAL PLANE OF LIDAR SCANNING

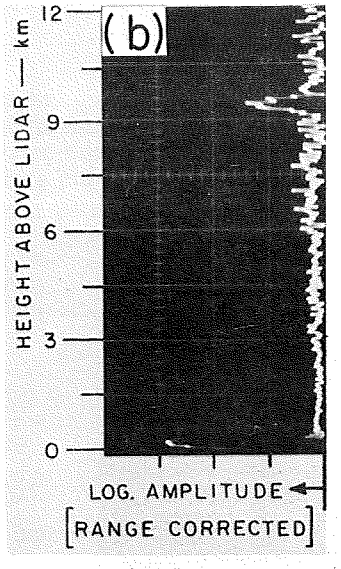

(b) SINGLE LIDAR TRACE (10 μs/cm) OF (RANGE-CORRECTED) LOG AMPLITUDE VERSUS RANGE (90° ELEVATION ANGLE)

FIGURE 25 DATA ON ATMOSPHERIC STRUCTURE OBTAINED BY AUTOMATED LIDAR SYSTEM IN THE LEE OF MT. ROSE, NEVADA, ON 12 FEBRUARY 1971, 08:20-08:27 PST

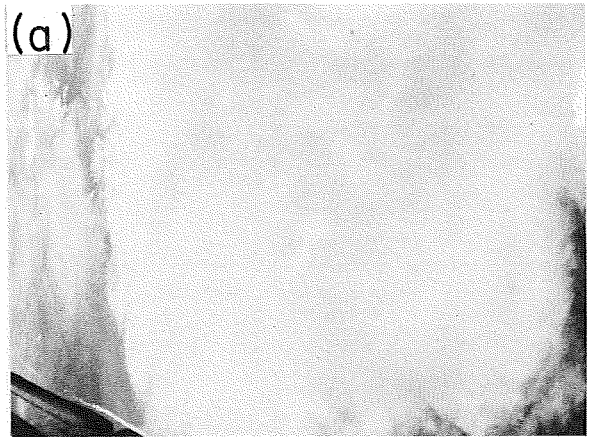

(a) PHOTOGRAPH OF OBSERVED CLOUD COVER

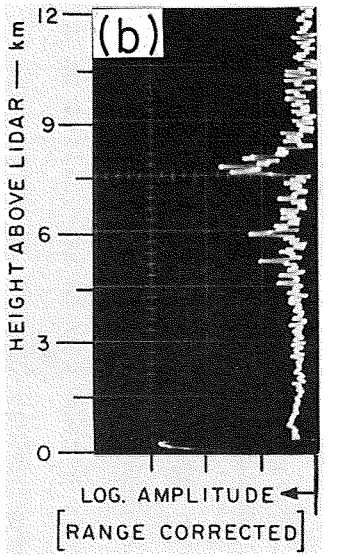

(b) SINGLE LIDAR TRACE (10 μs/cm) OF (RANGE-CORRECTED) LOG AMPLITUDE VERSUS RANGE (90° ELEVATION ANGLE)

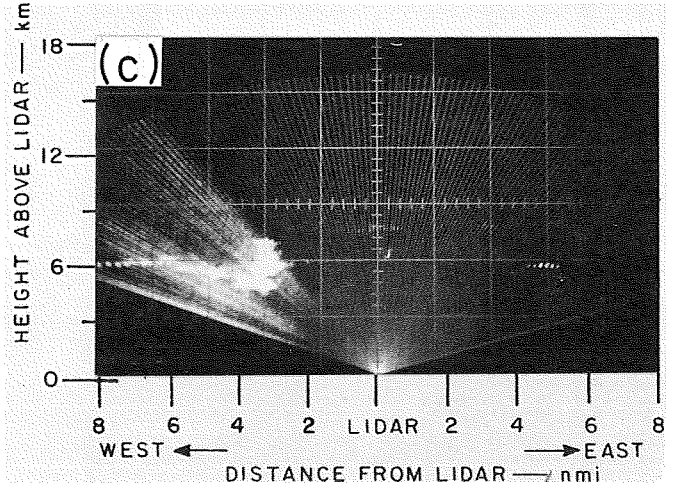

(c) INTENSITY-MODULATED CRT PRESENTATION OF ATMOSPHERIC STRUCTURE IN THE VERTICAL PLANE OF LIDAR SCANNING

FIGURE 26 DATA ON ATMOSPHERIC STRUCTURE OBTAINED BY AUTOMATED LIDAR SYSTEM IN THE LEE OF MT. ROSE, NEVADA, ON 12 FEBRUARY 1971, 14:00-14:07 PST

in elevation angle while scanning from Mt. Rose in the west toward the east. Multiple-layered structure in observed cirrus clouds is evident in all cases. The occasional brightness recorded in the direction of Mt. Rose (e.g., Figures 21 and 23) is due to the high sky background level near the position of the sun. The fractocumulus clouds observed on 10 February 1971 at 14:10 PST (Figure 23) are clearly portrayed in the RHI display at 1800 m above the lidar. In Figure 25, the lidar shows a distinct slope in the echo pattern recorded from an isolated patch of cirrus with virga. Numerous echoes can be identified at a height of 9 km above the lidar (approximately 35,000 ft MSL). These echoes must represent subvisible ice crystal clouds. Figure 25(b) shows a lidar backscatter signal from these clouds obtained by pointing the lidar at the zenith (90° elevation angle).

Although no appreciable wave action was present during the observation periods, the lidar data clearly demonstrate the superior performance of the system in mapping atmospheric structure.

VI RECOMMENDATIONS

As described in the Summary and Conclusions (Section II above), the application of the lidar technique to the observation and study of mountain waves and associated turbulence has been demonstrated. In particular, the principles and methods of operation have been worked out for a series of experimental lidar systems, and we have arrived at a point at which lidar can clearly be recognized as an important tool for research concerning mountain waves.

The following explicit recommendations are offered:

(1) That further observational studies using the Mark VIII lidar, or a comparable system, be made to obtain a more comprehensive data base that it has been possible to acquire in the largely evolutionary work accomplished to date.

(2) That in any study of mountain-wave dynamics, of the cloud physics involved, or of the associated low Richardson numbers and turbulence, a lidar of a type comparable to the Mark VIII system described in this report be considered as an essential component of the observational facilities. In particular, where aircraft are used to probe specific features of mountain waves, we believe that a lidar provides a valuable tool for directing the aircraft's operations. Without the information that the lidar can now graphically provide in near real time, much of the significant short-term variability of the waves does not become apparent until the occasion has passed and the aircraft data have been collected and analyzed.

REFERENCES

Alaka, M. A., "The Airflow over Mountains," Technical Note No. 34, World Meteorological Organization, Geneva, Switzerland (1960).

Atlas, D., J. I. Metcalf, J. H. Richter, and E. E. Gossard, "The Birth of CAT and Microscale Turbulence," J. of Atm. Sc., Vol. 27, No. 6, pp. 903-913 (September 1970).

Collis, R. T. H., "Lidar Detection of CAT " Astronautics and Aeronautics, pp. 52-55 (December 1964).

Collis, R. T. H., F. G. Fernald, and J. Alder, "Lidar Observations of Sierra Wave Conditions," J. Appl. Meteorol., Vol. 7, No. 2, pp. 227-233 (April 1968).

Corby, G. A., "The Airflow over Mountains; A Review of the State of Current Knowledge," Quart. J. Met. Soc., Vol. 80, No. 346, pp. 491-523 (1954).

Foldvik, A., and M. G. Wurtele, "The Computation of the Transient Gravity Wave," Geophys. J. R. Astr. Soc., Vol. 13, pp. 167-185 (1967).

Harrison, H. T., and D. F. Sowa, "Mountain Wave Exposure on Jet Routes," UAL Meteorology Circular No. 60 (1 February 1966).

Holmboe, J., and H. Klieforth, "Investigations of Mountain Lee Waves and the Airflow over the Sierra Nevada," Final Report, Contract No. AF19(604)-728, Department of Meteorology, University of California, Los Angeles, California (March 1957).

Kuettner, J. P., and D. K. Lilly, "Lee Waves in the Colorado Rockies," Weatherwise, Vol. 21, No. 5 (October 1968).

Long, R. R., "Some Aspects of the Flow of Stratified Fluids," Tellus, Vol. 5, pp. 42-58 (February 1953).

Reiter, E. R., and H. P. Foltz, "The Prediction of Clear Air Turbulence over Mountainous Terrain," J. of Appl. Meteorol., Vol. 6, No. 3, pp. 549-556 (June 1967).

Roach, W. T., "On the Influence of Synoptic Development on the Production of High Level Turbulence," Quart. J. R. Met. Soc., Vol. 96, No. 409, pp. 413-429 (1970).

Scorer, R. S., and H. Klieforth, "Theory of Mountain Waves of Large Amplitude," Quart. J. Royal Meteorol. Soc., Vol. 85, No. 364, pp. 131-143 (April 1959).

Sekera, Z., "Helmholtz Waves in a Linear Temperature Field with Vertical Wind Shear," J. Meteorol., Vol. 5, pp. 93-102 (June 1948).

Viezee, W., "An Investigation of Mountain Waves with Lidar Observations," Scientific Report 1, Contract NAS1-8933, for NASA, Langley Research Center, Stanford Research Institute, Menlo Park, California (January 1970).

Wooldridge, G., and P. F. Lester, "Detailed Observations of Mountain Lee Waves and A Comparison with Theory," Atmospheric Science Paper No. 138, Dept. of Atm. Sc., Colorado State University, Fort Collins, Colorado (March 1969).

Wurtele, M. G., "Meteorological Conditions Surrounding the Paradise Airline Crash of 1 March 1964," J. Appl. Meteorol., Vol. 9, No. 5, pp. 787-795 (October 1970).